

# Waveforming: An Overview With Beamforming

Qinyi Xu, *Student Member, IEEE*, Chunxiao Jiang, *Senior Member, IEEE*, Yi Han, Beibei Wang, *Senior Member, IEEE*, and K. J. Ray Liu, *Fellow, IEEE*

**Abstract**—By leveraging the natural multipath propagation of electromagnetic waves, waveforming is proposed as a promising paradigm that treats each multipath component in a wireless channel as a virtual antenna to exploit the spatial diversity. As the most commonly known waveforming technique for wideband systems, the time-reversal (TR) signal transmission produces a TR resonance by coherently combining multipath energy distributed on virtual antennas, and thus boosts the received signal strength while reducing interference. The wideband waveforming is, in many ways, similar to the multiple-input multiple-output (MIMO) beamforming, where multiple antennas are deployed to imitate a multipath transmission when the bandwidth is limited. In this paper, we provide an overview of recent advances on the wideband waveforming, including massive multipath effect, optimal resource allocation, wireless power transfer and secrecy enhancement for secured communications, and compare with the corresponding counterparts of traditional MIMO beamforming.

**Index Terms**—Waveforming, time-reversal (TR), multiple-input multiple-output (MIMO), beamforming.

## I. INTRODUCTION

THE NATURE provides a large number of degrees of freedom by means of radio multipath propagation. As the transmit signal encounters different scatterers in the environment and thus travels through different paths during its propagation, the channel between each transmitter (TX) and receiver (RX) antenna is a multipath channel.

Because an attenuated copy of the original signal is generated and transmitted through a different path when the transmit signal gets reflected or scattered by a scatterer, each scatterer in the environment can be viewed as a virtual antenna that transmits directly to the RX, in addition to the TX. Moreover, the channel characteristics between the virtual antenna and the RX antenna are determined by both of the radio paths between the TX and the scatterer and between the scatterer and the RX. An illustration of scatterers as virtual antennas in a multipath propagation environment is depicted in Fig. 1, where the

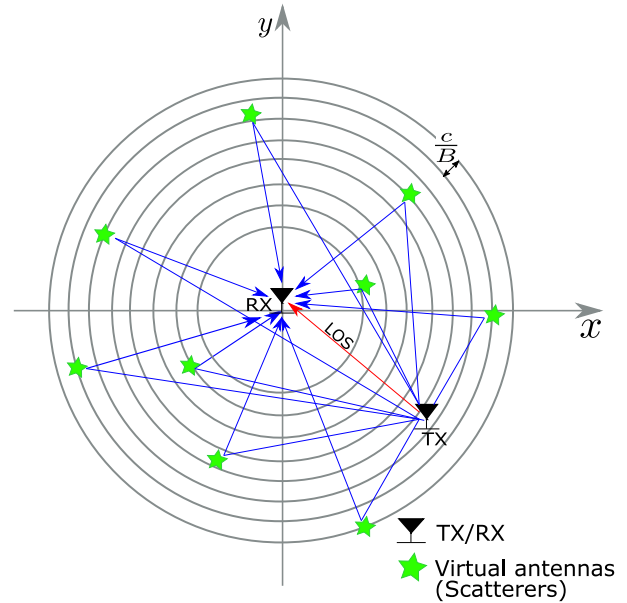


Fig. 1. Illustration of virtual antennas.

red arrow represents the line-of-sight (LOS) path and the blue arrows represent paths reflected and scattered by scatterers. Green stars in Fig. 1 represent scatterers in the environment, which can be viewed as virtual antennas that transmit an attenuated signal to the RX. All paths together form a multipath channel between the TX and the RX.

How to control the harvested multipaths as virtual antennas to achieve desired application purposes? *Waveforming* [1]–[6] has been proposed as a novel technique to control virtual antennas distributed in the environment to take advantages of the spatial diversity and thus achieve a high degree of freedom. When the bandwidth increases, more uncorrelated multipath components are revealed and thus higher degrees of freedom can be achieved for higher data rates and more reliable communications. The most well-known waveforming technique is the time-reversal (TR) signal transmission that has been considered as a novel paradigm for wideband systems, which treats each multipath component in a multipath channel as a virtual antenna [1]. The TR technique was originally designed for acoustics and ultrasound applications [7]–[10], and recent studies have been focused on TR wireless communications [11]–[16]. The TR signal transmission can be easily extended to multiple-antenna scenario [17]–[20], and the orthogonal frequency division multiplexing (OFDM) system [21].

Manuscript received April 11, 2017; revised July 16, 2017; accepted August 29, 2017. Date of publication September 8, 2017; date of current version February 26, 2018. (*Corresponding author: Qinyi Xu.*)

Q. Xu, B. Wang, and K. J. R. Liu are with the University of Maryland, College Park, MD 20742 USA, and also with Origin Wireless Inc., Greenbelt, MD 20770 USA (e-mail: qinyixu@umd.edu; bebewang@umd.edu; kjrlu@umd.edu).

C. Jiang was with the University of Maryland, College Park, MD 20742 USA, and also with Origin Wireless Inc., Greenbelt, MD 20770 USA. He is now with the Tsinghua Space Center, Tsinghua University, Beijing 100084, China (e-mail: chx.jiang@gmail.com).

Y. Han is with Origin Wireless, Inc., Greenbelt, MD 20770 USA (e-mail: yi.han@originwireless.net).

Digital Object Identifier 10.1109/COMST.2017.2750201

By leveraging virtual antennas in a constructive way, TR signal transmission can provide a significant spatial diversity gain and exhibit a TR resonance phenomenon [1], [22], [23]. Inspired by the TR technique, with certain objectives, the waveform design optimally weighs each virtual antenna in a multipath channel and combines the weighted signal from different paths at the receiver. Many works have been focused on optimal waveform design with different optimization criteria, such as interference cancellation, multi-user fairness and efficient wireless power transfer [2]–[6], [24]. Waveforming can be designed to address the interference problem which becomes a bottleneck limiting the system performance with the explosion of wireless traffic and the increase in the number of users in 5G.

In fact, the wideband waveforming is similar to the multiple-input multiple-output (MIMO) beamforming. When the bandwidth is too limited to resolve independent multipaths, MIMO was proposed to intimate a multipath transmission with multiple TX antennas or/and multiple RX antennas, such that high data rate transmission can be provided by exploiting a spatial diversity gain and a spatial multiplexing gain [25]–[27]. It has been widely deployed in wireless communication standards including WiFi, 3G and Long-Term Evolution (LTE). In recent years, studies on MIMO systems with a very large number of antennas at the base station (BS), a.k.a. massive MIMO, have shown its potential in reducing inter-user interference (IUI), and providing quasi-orthogonal channels and enormous enhancement in spectral efficiency and power efficiency [28]. Hence, as pointed out in [29] and [30], massive MIMO technology becomes one of the “big three” technologies for 5G, along with ultra-densification and millimeter wave (mmWave). However, massive MIMO also brings up several critical challenges, such as high complexity of hardware, high power consumption, high cost of deploying the massive number of antennas, antenna coupling effect, and difficulty in analog front end design as well as indoor deployment [31].

In multi-user MIMO systems, beamforming has become a widely used technique that utilizes multiple antennas to form a directional transmission beam pattern, to alleviate IUI. Beamforming can be viewed as a spatial filter which essentially weighs and sums signals from different TX antennas, such that the desired signal is added coherently at the receiver side [32]. The most common beamforming methods include maximal ratio combining (MRC), zero-forcing (ZF) and minimal mean square error (MMSE). Optimal beamforms can be designed with specific objectives. For example, studies on MIMO beamforming have been conducted thoroughly for optimal resource allocation problems when taking into consideration either the network throughput maximization or the multi-user fairness [33], [34]. Moreover, optimal beamforms have been designed for wireless powered communications to achieve a high-efficiency power transfer, and the optimal simultaneous information and energy delivery [35]–[38]. Recently, optimal beamforming has been investigated in secured communications where artificial noise is transmitted to degrade eavesdropper’s channel with the purpose of not impairing the information delivered to intended receivers [39]–[42].

This work aims to overview the advances in the wideband waveforming and show that it is indeed a dual problem

by illustrating its similarities with the well-known narrow-band MIMO beamforming, through problems on optimal resource allocation for multi-user wireless communications, wireless power transfer (WPT) and secured communications. In addition, the mathematical models for both systems are studied and compared, considering both the similarities and differences between physical antennas and virtual antennas.

This paper is organized as follows. In Section II, system models for the narrowband MIMO downlink system and the wideband downlink system are introduced and compared. The similarity and difference between physical antennas in the narrowband MIMO system and virtual antennas exploited from wideband multipath propagation are discussed. TR signal transmission as the first waveforming technique in wideband communications is introduced in Section III. In Section IV, we investigate various problems in both the narrowband MIMO beamforming and the wideband waveforming to improve the quality-of-service (QoS), including sum-rate maximization, max-min optimization and providing robustness. In Section V, how to design optimal beamforming and waveforming in the wireless power transfer is discussed for both systems. The MIMO beamforming and the wideband waveforming which utilize the artificial noise for secrecy enhancement in wireless communications are discussed in Section VI. Conclusion is drawn in Section VII.

## II. SYSTEM MODEL

In this section, we introduce and compare the system models for narrowband MIMO downlink transmission and wideband downlink transmission. In the MIMO system, beamforming is applied to create a directive transmission pattern by adjusting the weight in each physical antenna. Instead of using multiple transmit antennas at the BS, the wideband waveforming system treats each multipath component in the wireless channel as a virtual antenna. Each multipath component is related to a scatterer or a reflector in the environment, which can be resolved by a large bandwidth. In order to achieve a spatial selectivity in the wideband system, waveforming technique is used to adjust the weight on each multipath component, a.k.a., virtual antenna.

### A. Bandwidth vs Multipath

The multipath can be effectively harvested by adjusting transmission power and bandwidth [31], [43]. On one hand, a higher transmission power can lead to a higher signal-to-noise ratio (SNR). Consequently, the higher the transmission power is, the more observable multipath components are. On the other hand, the spatial resolution in resolving independent multipath components, i.e., the resolution to separate radio paths with different lengths in a multipath propagation, is limited by  $c/B$  as marked in Fig. 1, with  $c$  being the speed of light and  $B$  being the bandwidth. Therefore, the larger the bandwidth is, the better the spatial resolution is and thus the more multipaths can be revealed. The mathematical explanation of the relationship between bandwidth and multipath resolution is as follows.

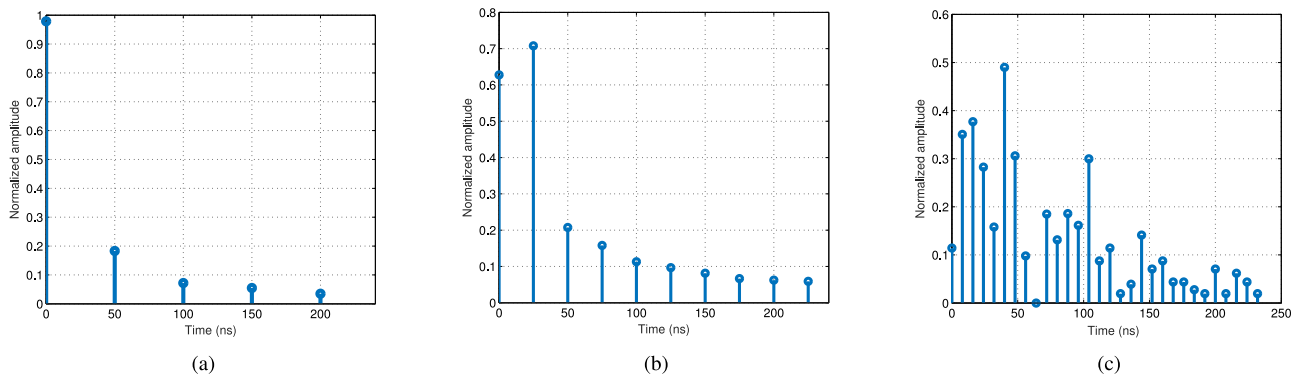


Fig. 2. Multipath channel vs bandwidth. (a) Measured channel under 20 MHz bandwidth (LTE standard). (b) Measured channel under 40 MHz bandwidth (the IEEE 802.11n standard). (c) Measured channel under 125 MHz bandwidth (entire ISM 5G band).

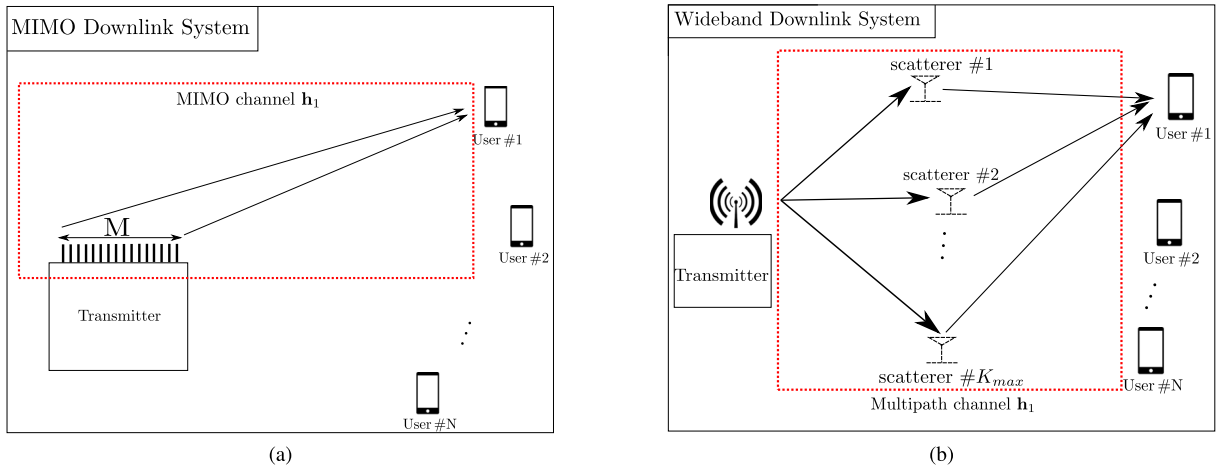


Fig. 3. Comparison on the system model. (a) MIMO downlink system. (b) Wideband waveforming downlink system [31].

In an environment with  $K_{max}$  independent multipath components existing between the TX and the RX, the continuous-time multipath channel  $h(t)$  is defined as collections of different radio propagation paths, i.e.,  $h(t) = \sum_{k=1}^{K_{max}} \alpha_k \delta(t - \tau_k)$ , where  $K_{max}$  is the number of scatterers in the wireless transmission medium.  $\alpha_k$  is the multipath coefficients of scatterer  $k$ , and  $\tau_k$  is the time delay associated with  $\alpha_k$ . The function  $\delta(\cdot)$  is the delta function. Note that, the delay spread of the wideband channel is  $\tau = \max_k \tau_k$ .

However, due to the limited bandwidth  $W$ , the estimated discrete-time channel  $\mathbf{h}$  at the receiver side is a sampled version of  $h(t)$ , i.e.,  $h[l] = \int_{l-1}^l P(\frac{l}{W} - t)h(t)dt$ , where  $P(\cdot)$  is the window function with length  $1/W$ . Given a delay spread  $\tau$ , when  $W \leq 1/\tau$ , only a single tap is resolved as the integration of all multipaths. When  $W > 1/\tau$ , multipath signals received within  $1/W$  seconds will be integrated into a single tap signal. Consequently, all multipaths can be resolved when  $W > 1/\Delta\tau_{min}$ , where  $\Delta\tau_{min}$  represents the smallest difference in time-of-flight (ToF) of consecutively received multipath signals. Because signals with ToF difference equal to or larger than  $1/W$  can be separated under a bandwidth  $W$ , a larger bandwidth enables a higher sampling rate to sample analog signals received from different paths and resolve more multipath components. Therefore, the number of resolved channel

taps, i.e., length of vector  $\mathbf{h}$ , is determined by  $L = \text{round}(\tau W)$ , as long as  $K_{max}$  is large enough to provide enough multipaths whose time delay difference  $\Delta\tau_{min}$  is close to 0.

Multipath channels captured under three different bandwidths at the same location in a rich-scattering environment are plotted and compared in Fig. 2, demonstrating the relationship between bandwidth and multipath resolution. Comparing Fig. 2a, Fig. 2b, and Fig. 2c, it is noticed that more multipaths and better resolution are resolved when the bandwidth increases. Therefore, the larger the bandwidth is, the better the spatial resolution is and thus the more multipaths can be revealed. In the LTE standard the bandwidth is 20MHz, and in WiFi (the IEEE 802.11n standard) systems the bandwidth is 40 MHz. Moreover, the entire industrial, scientific, and medical radio (ISM) 5G band occupies a total of 125MHz bandwidth. As projected in 5G, high carrier frequencies with larger bandwidths will be adopted in the future wireless communication systems [29], which makes the multipath channel of a good spatial resolution feasible.

### B. Narrowband MIMO System

We consider a single cell multi-user narrowband MIMO downlink system with  $M$  antennas at the BS and  $N$  users each equipped with a single receive antenna. The system model

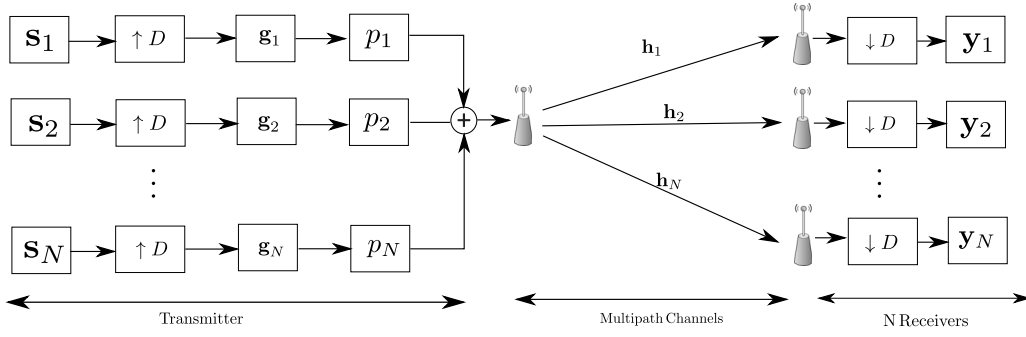


Fig. 4. Demonstration of wideband downlinks.

is illustrated in Fig. 3a. Due to the narrowband transmission, each link between a pair of TX and RX antenna is a single-tap channel, i.e., a scalar as the channel coefficient. The channel matrix is defined as the collection of channel vectors from all users:

$$\mathbf{H} = [\mathbf{h}_1^T, \mathbf{h}_2^T, \dots, \mathbf{h}_j^T, \dots, \mathbf{h}_N^T]^T \quad (1)$$

where  $\mathbf{H} \in \mathbb{C}^{N \times M}$  is an  $N \times M$  MIMO channel matrix,  $(\cdot)^T$  denotes the transpose operation.  $\mathbf{h}_j$  is the channel vector for user  $j$ ,  $\mathbf{h}_j = [h_{1j}, h_{2j}, \dots, h_{ij}, \dots, h_{Mj}]$ , where  $h_{ij} \in \mathbb{C}$  represents the channel coefficient from antenna  $i$  to user  $j$  and each coefficient is independently and identically distributed (i.i.d.).

In the multi-user MIMO downlink system, the received signal  $\mathbf{Y}$  at the receiver side can be modeled as

$$\mathbf{Y} = \mathbf{H}\mathbf{G}\mathbf{s} + \mathbf{n} \quad (2)$$

where  $\mathbf{s} \in \mathbb{C}^{N \times 1}$  is the transmit signal vector, i.e.,  $\mathbf{s} = [s_1, s_2, \dots, s_i, \dots, s_N]^T$ .  $\mathbf{n} \in \mathbb{C}^{N \times 1}$  is the additive white Gaussian noise vector with zeros mean and variance  $\sigma^2$ , and  $\mathbf{G} \in \mathbb{C}^{M \times N}$  is the MIMO beamforming matrix defined as  $\mathbf{G} = [\mathbf{g}_1, \mathbf{g}_2, \dots, \mathbf{g}_j, \dots, \mathbf{g}_N]$ . Moreover,  $\mathbf{g}_j$  in  $\mathbf{G}$  is the antenna weight vector for user  $j$ , and  $\|\mathbf{g}_j\|_2^2 = p_j$  where  $\|\cdot\|_2$  denotes the L2-norm of a vector. In the following, to simplify notation, we assume  $\|\mathbf{g}_j\|_2^2 = 1$  and each user has a power allocation factor  $p_j$  without loss of generality.

To further analyze the received signal in (2), we take user  $j$  for an example with its received signal expressed as

$$y_j = \sqrt{p_j} \mathbf{h}_j \mathbf{g}_j s_j + \sum_{\substack{i=1 \\ i \neq j}}^N \mathbf{h}_j \sqrt{p_i} \mathbf{g}_i s_i + n_j, \quad \forall j \quad (3)$$

where  $p_j$  represents the transmit power assigned to user  $j$ , and  $n_j$  is the additive white Gaussian noise with  $n_j \sim \mathcal{CN}(0, \sigma^2)$  for user  $j$ . It is seen from (3) that the received signal consists of desired signal component and IUI component as listed in Table I.

### C. Wideband Waveforming System

In this part, we consider a wideband downlink system with  $N$  users and an illustration of the system is plotted in Fig. 3b. With a large bandwidth, channels in the wideband waveforming system possess multiple taps, due to the multipath propagation. The channel between the BS and user  $j$  is defined

as  $\mathbf{h}_j = [h_j[1], h_j[2], \dots, h_j[L], \dots, h_j[L]]^T$ , where  $h_j[l] \in \mathbb{C}$  is a scalar representing the wideband channel coefficient on tap  $l$  for user  $j$ , and each coefficient is independent but not identically distributed.

A diagram shown in Fig. 4 demonstrates how a wideband waveforming system works in the downlink transmission. During the downlink transmission, the information  $s_j$  to be transmitted to receiver  $j$  is first up-sampled by a rate back-off factor  $D$  to match the baud rate with the sampling rate [1]. Then the real transmit signal is defined as  $s_j^{[D]}[k] = s_j[n]$  if  $k = nD$ , and  $s_j^{[D]}[k] = 0$  otherwise.

Afterwards, the upsampled version of transmit signal is convolved with the waveforming vector  $\mathbf{g}_j$  and multiplied with a power coefficient  $p_j$ , before combined with other users downlink transmit signal.  $\mathbf{g}_j \in \mathbb{C}^{L \times 1}$  is the waveforming vector for user  $j$ , i.e., the time-domain multipath weight vector, with  $\|\mathbf{g}_j\|_2 = 1$ .

At the receiver side, the received signal of user  $j$  is first downsampled by  $D$ , and then it can be written as a vector  $\mathbf{y}_j$  as

$$\begin{aligned} y_j[m] &= \left( \mathbf{H}_j \left( \sum_{i=1}^N \sqrt{p_i} s_i^{[D]} * \mathbf{g}_i \right) \right) [Dm] + n_j[m] \\ &= \sqrt{p_j} \mathbf{H}_j \left( \left\lfloor \frac{L-1}{D} \right\rfloor + 1 \right) \mathbf{g}_j s_j \left[ m - \left\lfloor \frac{L-1}{D} \right\rfloor - 1 \right] \\ &\quad + \sqrt{p_j} \sum_{\substack{k=1 \\ k \neq \left\lfloor \frac{L-1}{D} \right\rfloor + 1}}^{2 \left\lfloor \frac{L-1}{D} \right\rfloor + 1} \mathbf{H}_j^{(k)} \mathbf{g}_j s_j [m - k] \\ &\quad + \sum_{k=1}^{2 \left\lfloor \frac{L-1}{D} \right\rfloor + 1} \mathbf{H}_j^{(k)} \left( \sum_{\substack{i=1 \\ i \neq j}}^N \sqrt{p_i} \mathbf{g}_i s_i [m - k] \right) + n_j[m] \quad (4) \end{aligned}$$

where  $\mathbf{H}_j$  is a  $(2 \left\lfloor \frac{L-1}{D} \right\rfloor + 1) \times L$  Toeplitz convolution matrix generated from  $\mathbf{h}_j$  as shown in (5), as shown at the bottom of the next page.  $\mathbf{H}_j^{(k)}$  is the  $k^{\text{th}}$  row of matrix  $\mathbf{H}_j$ .  $n_j[m]$  is the additive white Gaussian noise with  $n_j[m] \sim \mathcal{CN}(0, \sigma^2)$ .

As can be seen from (4), the received signal contains desired signal parts, interference signals from ISI and IUI, along with noise, which are listed in Table I.

TABLE I  
SUMMARY ON SYSTEM MODEL

	MIMO Downlink System	Waveforming Downlink System
<b>Signal</b>	$y_j$ in (3)	$y_j[m]$ in (4)
<b>Single User Channel</b>	$\mathbf{h}_j$ : $1 \times M$ vector	$\mathbf{H}_j$ : $\left(2\lfloor \frac{L-1}{D} \rfloor + 1\right) \times L$ matrix
<b>All Users' Channel</b>	$\mathbf{H}$ in (1)	$\mathbf{Q}$ in (6)
<b>Desired Signal</b>	$\sqrt{p_j} \mathbf{h}_j \mathbf{g}_j s_j$	$\sqrt{p_j} \mathbf{H}_j^{\left(\lfloor \frac{L-1}{D} \rfloor + 1\right)} \mathbf{g}_j s_j \left[m - \lfloor \frac{L-1}{D} \rfloor - 1\right]$
<b>IUI</b>	$\sum_{i=1, i \neq j}^N \mathbf{h}_j \sqrt{p_i} \mathbf{g}_i s_i$	$\sum_{k=1}^{2\lfloor \frac{L-1}{D} \rfloor + 1} \mathbf{H}_j^{(k)} \left(\sum_{i=1, i \neq j}^N \sqrt{p_i} \mathbf{g}_i s_i [m - k]\right)$
<b>ISI</b>		$\sqrt{p_j} \sum_{k=1, k \neq \lfloor \frac{L-1}{D} \rfloor + 1}^{2\lfloor \frac{L-1}{D} \rfloor + 1} \mathbf{H}_j^{(k)} \mathbf{g}_j s_j [m - k]$

Meanwhile, the channel matrix of all users is defined as

$$\mathbf{Q} = \left[ \mathbf{H}_1^T, \mathbf{H}_2^T, \dots, \mathbf{H}_j^T, \dots, \mathbf{H}_N^T \right]^T \quad (6)$$

where  $\mathbf{Q}$  is an  $N(2\lfloor \frac{L-1}{D} \rfloor + 1) \times L$  matrix.

Unlike the MIMO beamforming which relies on multiple physical antennas for high degrees of freedom, in the wideband waveforming system ample degrees of freedom are provided by the nature where a fine-grained multipath channel is available with a large bandwidth. In practise, each antenna in a wireless communication system requires an independent radio-frequency (RF) chain which includes a low-noise amplifier, an up/down converter, intermediate-frequency amplifier, an analog-to-digital (A/D) or digital-to-analog (D/A) converter and some bandpass filters. Because multiple antennas are deployed, the cost and complexity to implement a MIMO beamforming system are much higher than those of a single-antenna wideband system. Hence, waveform design succeeds in making the wideband waveforming system outstanding for future wireless communications by supporting high data rate and reliable services, but with a simple and low-cost hardware implementation.

On the other hand, waveforming can be utilized to detect and track the changes in a multipath propagation environment with a high accuracy and has been proposed for green Internet of Things (IoT) applications, e.g., indoor locationing that achieves a centimeter level accuracy [44]–[46], indoor speed estimation [47], through-the-wall event detection [48], human recognition [49] and breathing rate estimation [50]. Considering its capability in wireless communications and

wireless sensing, waveforming will be a promising technology for 5G and future IoT applications, and deserves a thorough study.

We summarize this section and compare the system model between the MIMO downlink system and the waveforming downlink system in Table I.

### III. TIME-REVERSAL SIGNAL TRANSMISSION

In this section, the details of TR signal transmission are discussed and related works are reviewed.

#### A. History of TR Signal Transmission

TR signal processing technique is originally proposed in 1957 to compensate the delay distortion in picture transmission [51]. Then, its applications in acoustic communications has been studied, and it is validated through a series of theoretical and experimental works that the energy of the TR acoustic wave is only focused at the intended locations [7], [8], [10], [52]–[57].

Later, applications of TR technique in wireless communications have received an increasing attention. In [12] and [58]–[63], the study of TR signal transmission has been extended to applications related to the electromagnetic (EM) field, which demonstrates the TR resonance through experiments and justifies the assumption of channel stationarity and channel reciprocity given that the coherence time is long enough. Meanwhile, the performance of ultra-wideband (UWB) communication system with TR signal transmission has been studied in [11], [13]–[15], and [64]. To further

$$\mathbf{H}_j = \begin{pmatrix} h_j \left[ L - D \left\lfloor \frac{L-1}{D} \right\rfloor \right] & \dots & \dots & 0 \\ \vdots & \vdots & \ddots & \vdots \\ h_j[L-D] & h_j[L-1-D] & \dots & 0 \\ h_j[L] & h_j[L-1] & \dots & h_j[1] \\ 0 & 0 & \dots & h_j[1+D] \\ \vdots & \vdots & \ddots & \vdots \\ 0 & 0 & \dots & h_j \left[ 1 + D \left\lfloor \frac{L-1}{D} \right\rfloor \right] \end{pmatrix} \quad (5)$$

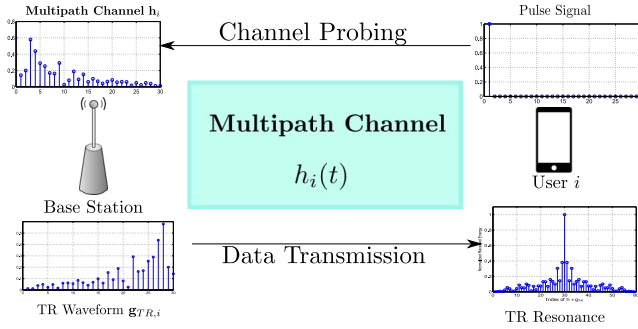


Fig. 5. Demonstration of TR signal transmission.

utilize the spatial diversity provided by transmission through multiple antennas, TR signal transmission has been extended to work with MIMO technology [12], [17]–[20]. Moreover, a TR based OFDM system where wideband frequency-selective channels are decomposed into independent narrowband subchannels and TR is applied as a precoding method has been studied in [21].

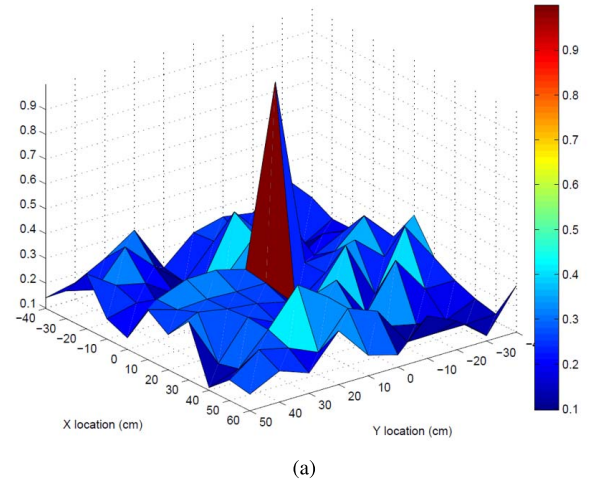
Recently, experiments as well as theoretic analysis have been conducted to illustrate the potential of TR for future green communications [1], [16]. It was shown that a typical TR receiver can achieve over an order of magnitude in power reduction and interference alleviation [1]. Later on, the concept of time-reversal division multiple access (TRDMA) was proposed and a system-level performance analysis was provided in [22]. In TRDMA, users in a wideband system are separated by the inherent TR resonance and the ISI and IUI are reduced. In order to further improve the performance of TRDMA communication system, researches have been conducted to suppress interference by means of waveform design [2], [4], [6], and interference pre-cancellation algorithm [3], [5]. A device-to-device communication system based on TR signal transmission was proposed where the optimal power allocation is determined through a Stackelberg game [65]. The performance of a massive multipath TR communication system was studied in [31], where a comprehensive comparison between the massive MIMO system and the massive multipath TR system was conducted both theoretically and through simulations.

### B. How Does TR Work?

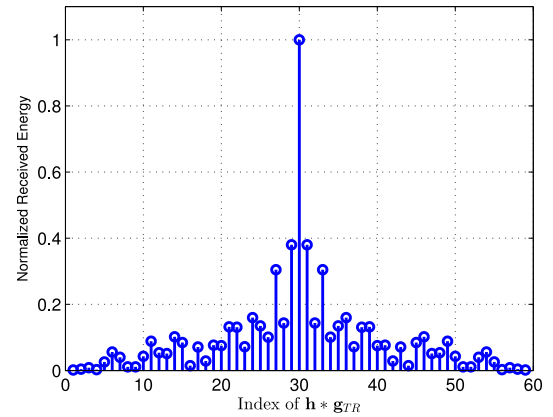
Let us consider a wideband downlink system depicted in Fig. 3b with  $N$  users. A typical TR signal transmission consists of two phases: 1) the channel probing phase, and 2) the data transmission phase, as shown in Fig. 5.

1) *Channel Probing Phase*: Before the BS transmits downlink signals to users, it needs to estimate each user's channel  $\mathbf{h}_i$ ,  $\forall i$  to generate TR waveforms. In order to estimate the CSI  $\mathbf{h}_i$  under bandwidth  $W$ , user  $i$  first sends out a pulse signal propagating through the continuous-time multipath channel  $h_i(t)$ . Afterwards, the BS obtained a discrete-time CSI estimation  $\mathbf{h}_i$ .

2) *Data Transmission Phase*: As shown in Fig. 4, during the downlink transmission, the discrete signal  $s_i$  is sent from the BS to user  $i$  after upsampling and convolving with the



(a)



(b)

Fig. 6. TR resonance. (a) The spatial focusing of TR resonance: received energy at different locations. (b) The temporal focusing of TR resonance: received energy at different sampling time ( $L = 30$ ).

TR waveform  $\mathbf{g}_{i,TR}$  that is defined as  $\mathbf{g}_{TR,i} = \mathbf{H}_i^{(\lfloor \frac{L-1}{D} \rfloor + 1)\dagger}$ , where  $(\cdot)^\dagger$  denotes the Hermitian operation, i.e., transpose and conjugate.

Then, according to (4), the received signal  $y_i[m]$  in a TR based wideband waveforming system can be written as follows.

$$\begin{aligned}
 y_i[m] = & \sqrt{p_i} \|\mathbf{h}_i\|_2^2 s_i \left[ m - \left\lfloor \frac{L-1}{D} \right\rfloor - 1 \right] \\
 & + \sqrt{p_i} \sum_{\substack{k=1 \\ k \neq \lfloor \frac{L-1}{D} \rfloor + 1}}^{2 \lfloor \frac{L-1}{D} \rfloor + 1} \mathbf{H}_i^{(k)} \mathbf{H}_i^{(\lfloor \frac{L-1}{D} \rfloor + 1)\dagger} s_i[m-k] \\
 & + \sum_{k=1}^{2 \lfloor \frac{L-1}{D} \rfloor + 1} \mathbf{H}_i^{(k)} \left( \sum_{\substack{j=1 \\ j \neq i}}^N \mathbf{H}_j^{(k)\dagger} \sqrt{p_j} s_j[m-k] \right) + n_i[m]
 \end{aligned} \tag{7}$$

Because of the TR resonance, energy in the desired signal is boosted by the TR resonating strength  $\|\mathbf{h}_i\|_2^2$ , while the energy

of both ISI and IUI term is typically much smaller. The details of the TR resonance are discussed in the following.

### C. TR Resonance

In a wireless communication system, ISI and IUI deteriorate the QoS of each individual user. On one hand, the spatial focusing effect of the TR resonance suppresses the energy leakage to other receivers and focuses most of the signal energy at the intended user. Consequently, TR signal transmission naturally reduces the required transmit power and lowers the IUI. As depicted in Fig. 6a, an example of the spatial focusing effect of the TR resonance is shown with an energy peak at the focused spatial location. On the other hand, due to the temporal focusing effect of the TR resonance which reduces the inter-symbol energy leakage, the ISI can be effectively reduced for high-speed broadband communication with the help of a large backoff factor  $D$ . In Fig. 6b, an example of the temporal focusing effect of the TR resonance is shown, where the received energy exhibits a strong peak at the time instance  $L$ , corresponding to  $\mathbf{h} * \mathbf{g}_{TR}[L]$ . In other words, the desired signal component in (7) is amplified, outstanding from ISI and IUI components.

*Remark 1:* The TR waveform is the MRC waveform for the wideband communication system [31]. As presented in [66], MRC is a technique to combine received signals from different transmit paths with a weight proportional to each signal strength which usually is the conjugated version of its corresponding channel coefficient. Consequently, strong signals are further amplified while weak signals are attenuated. Through TR waveforming, signals arrived from different virtual antennas, i.e., multipaths, are added up coherently by convoluting with its TR signature. This is equivalent to multiplying each copy of transmitted signal through different paths with its own conjugated channel coefficient. Hence, TR waveform becomes a MRC waveform.

Due to the fact that the number of resolved multipath components is proportional to the bandwidth, the resolution of TR resonance highly depends on bandwidth. Examples are depicted in Fig. 7a, 7b, 7c where the TR resonance under different bandwidths is investigated through simulation, and the studies based on real measurements are in Fig. 7d, 7e, 7f. It is obvious that when the bandwidth increases, the TR resonance has a spikier spatial focusing effect. Moreover, simulation results are consistent with those obtained from the real measured CSI.

*Remark 2:* In order to have a fine resolution for the TR resonance, a large bandwidth  $W$  is required to perceive enough independent multipath components in the environment.

Furthermore, we compare the TR waveforming and MIMO MRC beamforming, in terms of the spacial focusing of the received energy. As plotted in Fig. 7a, 7b, and in Fig. 7g, 7h, TR waveforming achieves a similar spatial focusing effect with MIMO MRC beamforming under a similar consuming bandwidth. Here, the consuming bandwidth is defined as the sum of the transmission bandwidth on each link. As shown by the focusing ball in Fig. 7c and Fig. 7i, when using a single TX antennas and 125 MHz bandwidth, TR waveforming

outperforms by achieving the similar spatial focusing effect with MIMO MRC beamforming where 100 TX antennas are deployed and each works under 2 MHz, i.e., a consuming bandwidth of 200 MHz.

### D. Massive Multipath Effect

In a wideband waveforming downlink system, channels from the single TX antenna to multiple single-antenna receivers at different locations form a channel matrix  $\mathbf{Q}$ , which is defined in (6). As shown in Fig. 7c, the high-resolution spatial focusing effect of TR resonance is supported by the following theorem of massive multipath effect [31].

*Theorem 1 (Massive Multipath Effect [31]):* Suppose in the channel matrix  $\mathbf{Q}$  all channels are normalized as  $\|\mathbf{H}_i^{(\lfloor \frac{L-1}{D} \rfloor + 1)}\|_2 = 1$  and the environment is rich with scatterers, i.e., a sufficiently large  $K_{max}$  is guaranteed. Then, when the bandwidth  $W$  goes to infinity such that it provides an extremely high resolution to resolve all multipath components, we have the following asymptotic behaviour for the channel matrix  $\mathbf{Q}$  as

$$\lim_{W \rightarrow \infty} \mathbf{Q}\mathbf{Q}^\dagger = \mathbb{I}_{N \times N} \quad (8)$$

where  $\mathbb{I}_{N \times N}$  represents an identity matrix with dimension  $N$ .

In other words, the multipath channels become mutually orthogonal if the bandwidth  $W$  to resolve multipath components is large enough under the rich multipath setting.

Similarly, the spatial pinpoint of the MIMO beamforming as depicted in Fig. 7i follows the massive MIMO effect [67], which shows that the channel matrix  $\mathbf{H}$  of a narrowband MIMO system exhibits an asymptotic behavior when the number of antennas increases. The details are as follows.

*Theorem 2 (Massive MIMO Effect [67]):* When the number of antennas  $M$  grows sufficiently large, the random matrix theory provides a central limit theorem for the distribution of the singular values of  $\mathbf{H}$ , and thus under the law of large numbers we can have

$$\lim_{M \rightarrow \infty} \frac{1}{M} \mathbf{H}\mathbf{H}^\dagger = \mathbb{I}_{N \times N} \quad (9)$$

where  $(\cdot)^\dagger$  denotes the Hermitian operation, i.e., transpose and conjugate, and  $\mathbb{I}_{N \times N}$  represents an  $N \times N$  identity matrix.

Although it provides the spatial-temporal TR resonating effect, TR waveforming cannot eliminate the ISI and IUI completely. The ISI could be very severe when the symbol duration is smaller than the channel delay spread. As a result, adjacent transmit symbols are contaminated by each other, especially when the transmit power is high. Moreover, because channels between different users locating at different locations are not orthogonal in reality, the IUI under TR waveforming is inevitable in a multi-user wideband waveforming system. Hence, waveform design is indispensable for improving the performance of wideband systems. The optimal waveforming can be designed according to specific performance metrics similar to the MIMO beamforming optimization.

With certain optimization criteria, common waveforming/beamforming methods include the MRC, the ZF and the MMSE [68]. With the objective to maximize the received

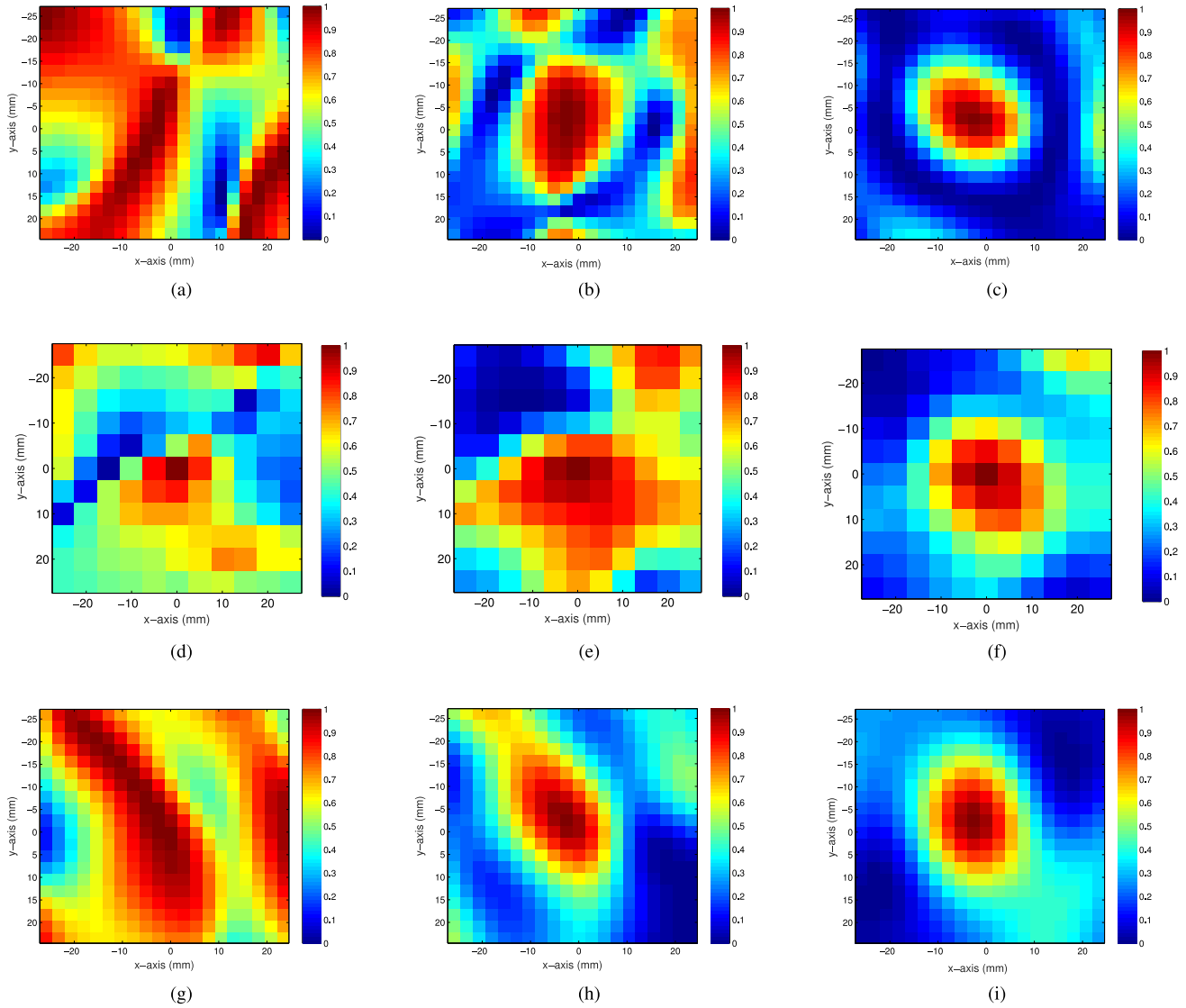


Fig. 7. Bandwidth vs TR resonance in spatial focusing. (a) The spatial focusing of TR resonance under 20 MHz bandwidth (simulation). (b) The spatial focusing of TR resonance under 40 MHz bandwidth (simulation). (c) The spatial focusing of TR resonance under 125 MHz bandwidth (simulation). (d) The spatial focusing of TR resonance under 20 MHz bandwidth (real measurement). (e) The spatial focusing of TR resonance under 40 MHz bandwidth (real measurement). (f) The spatial focusing of TR resonance under 125 MHz bandwidth (real measurement). (g) The MIMO MRC beamforming of 10 antennas under 2 MHz bandwidth (simulation). (h) The MIMO MRC beamforming of 20 antennas under 2 MHz bandwidth (simulation). (i) The MIMO MRC beamforming of 100 antennas under 2 MHz bandwidth (simulation).

signal-to-noise ratio (SNR), MRC method is proposed where signals from different transmit paths are summed at the receiver after being multiplied by weight factors proportional to the conjugated version of their corresponding propagation channel [66]. Through the MRC waveform/beamforming, signals are combined linearly and coherently such that strong signals are further amplified while weaker ones are attenuated. Consequently, the receiver signal-to-noise ratio (SNR) is maximized. With the objective to completely eliminate IUI, the ZF beamforming/waveforming has been designed such that the waveform or beamform of one user is orthogonal to other channels such that there is no energy leakage and thus no interference to other users [69]. In an estimation context, in order to minimize the estimate mean square error of the received signal, the MMSE beamforming/waveforming has been proposed [32]. The aforementioned beamform and

waveform design are listed in Table II, where  $\mathbf{H}$  is the channel matrix for all users in a MIMO system defined by (1) while  $\mathbf{Q}$  denotes that for a wideband waveform system as defined in (6).  $\mathbf{G}$  is the waveform/beamforming matrix for all users, and  $\mathbf{g}_j$  is the waveform for user  $j$ . Coefficients  $c_{MRC}$ ,  $c_{ZF}$  and  $c_{MMSE}$  are the normalized factors which guarantee the waveform and beamform to have unit energy. The vector  $\mathbf{e}_j$  is an elementary vector with  $l_j = (j-1)(2\lfloor \frac{L-1}{D} \rfloor + 1) + \lfloor \frac{L-1}{D} \rfloor + 1$ . The detailed comparison on waveform and beamforming are studied in the following sections.

#### IV. OPTIMAL RESOURCE ALLOCATION

In what follows, the joint problem of power allocation and waveform/beamforming design is studied with the objective

TABLE II  
TYPICAL BEAMFORMING VS WAVEFORMING

	Beamforming	Waveforming [31]
MRC	$\mathbf{G} = c_{MRC} \mathbf{H}^\dagger$	$\mathbf{g}_j = c_{MRC} \mathbf{H}_j^{(\lfloor \frac{L-1}{D} \rfloor + 1)^\dagger}$
ZF	$\mathbf{G} = c_{ZF} \mathbf{H}^\dagger (\mathbf{H} \mathbf{H}^\dagger)^{-1}$	$\mathbf{g}_j = \begin{cases} c_{ZF} \mathbf{Q}^\dagger (\mathbf{Q} \mathbf{Q}^\dagger)^{-1} \mathbf{e}_{l_j}, & \text{if } \mathbf{Q} \text{ full row rank} \\ c_{ZF} (\mathbf{Q}^\dagger \mathbf{Q})^{-1} \mathbf{Q}^\dagger \mathbf{e}_{l_j}, & \text{if } \mathbf{Q} \text{ full column rank} \end{cases}$
MMSE	$\mathbf{G} = c_M \mathbf{H}^\dagger (\mathbf{H} \mathbf{H}^\dagger + \frac{1}{p_u} \mathbb{I})^{-1}$	$\mathbf{g}_j = c_M \mathbf{Q}^\dagger (\mathbf{Q} \mathbf{Q}^\dagger + \frac{1}{p_u} \mathbb{I})^{-1} \mathbf{e}_{l_j}$

being the sum-rate maximization, max-min optimization, or providing robustness. Moreover, in this section, we use  $(\cdot)^*$  to denote an optimal solution.

#### A. Sum-Rate Maximization

One important QoS in a multi-user wireless communication system is the total throughput of the network, which is usually defined as the weighted sum-rate of all users. This kind of problem is usually formulated as a joint optimization of power allocation and transmit waveform/beamforming design, subject to a constraint on total transmit power.

One example of the joint problem can be written as

$$\begin{aligned} & \underset{\mathbf{p}, \mathbf{G}}{\text{maximize}} && \sum_{i=1}^N w_i \log(1 + \text{SINR}_i) \\ & \text{subject to} && \|\mathbf{p}\|_1 \leq P, p_i \geq 0, \\ & && \|\mathbf{g}_i\|_2 = 1, \forall i \end{aligned} \quad (10)$$

where  $\mathbf{p}$  is the power allocation vector with entry  $p_i$  as the downlink transmit power assigned to user  $i$ ,  $P$  is the total transmit power constraint, and  $\mathbf{g}_i$  is the transmit waveform/beamform of user  $i$ .  $\text{SINR}_i$  represents the received signal-to-interference-plus-noise ratio (SINR) of user  $i$  in the downlink transmission, which is a function of the power  $\mathbf{p}$  and the matrix  $\mathbf{G}$ . In order to allocate resources optimally, considering various quality-of-service (QoS) requirements or priorities for different users, weight factors  $w_i > 0, \forall i$  are introduced to the optimization problem as predefined hyperparameters to enable heterogeneity. If all users share a homogeneous QoS requirement or priority,  $w_i = 1$  for all users. Otherwise,  $w_i$  will be different for users with heterogeneous QoS requirements or priorities, and a high priority or QoS requirement corresponds to a large  $w_i$ . Consequently, in the optimal solution users associated with a larger weight  $w_i$  will be assigned with more resources to meet their own requirements. Since only the ratio between the weight factor and the sum of all weight factors, i.e.,  $w_i / \sum_{i=1}^N w_i$ , affects the optimal power allocation, there is no need to have a constraint on  $w_1 + w_2 + \dots + w_N = 1$ . Moreover, because the achievable rate of user  $i$  with bandwidth  $W_i$  is defined as  $W_i \log(1 + \text{SINR}_i)$  and  $W_i$  can be incorporated in the weight  $w_i$ , we assume  $W_i = 1$  in the objective function of (10) without loss of generality.

In the MIMO downlink system, according to the signal model in (3), the received  $\text{SINR}_i$  is defined as

$$\text{SINR}_i = \frac{p_i \mathbf{g}_i^\dagger \mathbf{h}_i^\dagger \mathbf{h}_i \mathbf{g}_i}{\sum_{\substack{j=1 \\ j \neq i}}^N p_j \mathbf{g}_j^\dagger \mathbf{h}_i^\dagger \mathbf{h}_i \mathbf{g}_j + \sigma^2} \quad (11)$$

where the only interference comes from IUI, and  $\mathbf{h}_i$  is the MISO channel vector between the multi-antenna BS and the single-antenna user  $i$ .

On the other hand, considering the existence of ISI and IUI, the definition of SINR in a multi-user wideband downlink system is different and given in (12), as shown at the top of the next page. In (12), inside the denominator, the term  $p_i \mathbf{g}_i^\dagger (\mathbf{H}_i^\dagger \mathbf{H}_i - \mathbf{H}_i^{(\lfloor \frac{L-1}{D} \rfloor + 1)^\dagger} \mathbf{H}_i^{(\lfloor \frac{L-1}{D} \rfloor + 1)}) \mathbf{g}_i$  accounts for the ISI of user  $i$ , and  $\sum_{j=1, j \neq i}^N p_j \mathbf{g}_j^\dagger \mathbf{H}_i^\dagger \mathbf{H}_i \mathbf{g}_j$  is the IUI energy.

*Remark 3:* As mentioned above, a back-off factor  $D$  is introduced in the wideband system to match rate and combat and eliminate the ISI resulted by the delay spread in a multipath channel. Hence, the actual rate  $R_j$ , i.e., the spectral efficiency, for user  $j$  in the wideband waveforming system is defined as  $R_j = \frac{1}{D} \log(1 + \text{SINR}_j)$  [22].

In (10), we combine the constant  $\frac{1}{D}$  into the weight factor  $w_i$  for the sake of a unified notation.

The solution to the joint optimization problem in (10) has been studied for both the MIMO downlink system [70] and the wideband downlink system [2]. In general, despite the different forms of SINR, the optimal power allocation vector  $\mathbf{p}^*$  and the optimal waveform or beamform  $\mathbf{G}^*$  for the weighted sum-rate maximization problem can be obtained through an iterative optimizing process, described as follows.

- 1) The problem is first converted into an uplink optimization through the downlink-uplink duality [71], and it becomes a maximization of the uplink sum-rate with uplink power allocation scheme  $\mathbf{q}$  and waveforming/beamforming scheme  $\mathbf{S}$ .
- 2) By fixing the uplink power allocation scheme  $\mathbf{q}$ , the optimal uplink waveforming/beamforming scheme  $\mathbf{S}$  that maximizes sum-rate can be optimized.
- 3) Given a waveform/beamform matrix  $\mathbf{S}$ , the best power allocation vector  $\mathbf{q}$  is optimized through the *water-filling* algorithm.
- 4) Iterate between step 2 and 3 until the solution converges, then the optimal downlink waveform/beamform is the  $\mathbf{G}^*$  obtained directly as the optimal uplink  $\mathbf{S}^*$ , and then

$$\text{SINR}_i = \frac{p_i \mathbf{g}_i^\dagger \mathbf{H}_i \left( \lfloor \frac{L-1}{D} \rfloor + 1 \right)^\dagger \mathbf{H}_i \left( \lfloor \frac{L-1}{D} \rfloor + 1 \right) \mathbf{g}_i}{p_i \mathbf{g}_i^\dagger \left( \mathbf{H}_i^\dagger \mathbf{H}_i - \mathbf{H}_i \left( \lfloor \frac{L-1}{D} \rfloor + 1 \right)^\dagger \mathbf{H}_i \left( \lfloor \frac{L-1}{D} \rfloor + 1 \right) \right) \mathbf{g}_i + \sum_{\substack{j=1 \\ j \neq i}}^N p_j \mathbf{g}_j^\dagger \mathbf{H}_i^\dagger \mathbf{H}_i \mathbf{g}_j + \sigma^2} \quad (12)$$

the downlink power allocation is optimized with  $\mathbf{G}^*$  and has a closed form.

*Remark 4:* Given a power allocation  $\mathbf{p}$ , the optimal waveform/beamform  $\mathbf{G}$  which maximizes the individual rate, has the same form as the MMSE waveform or beamform listed in Table II [2].

In the following, we briefly introduce three different optimization problems derived from the weighted sum-rate maximization in (10).

1) *Transmit Power Minimization:* In reality, the performance of a wireless communication system is limited by battery life which supports the transmission between the BS and users. In order to extend the working time of the system while maintaining a desired QoS, as the dual problem to (10), it has been proposed to minimize the total downlink transmit power under the constraint on the minimum of weighted sum-rate. The problem is written as follows.

$$\begin{aligned} & \underset{\mathbf{p}, \mathbf{G}}{\text{minimize}} && \|\mathbf{p}\|_1 \\ & \text{subject to} && \sum_{i=1}^N w_i \log(1 + \text{SINR}_i) \geq R_{sum}, \\ & && p_i \geq 0, \|\mathbf{g}_i\|_2 = 1, \forall i \end{aligned} \quad (13)$$

where  $\|\cdot\|_1$  denotes the L1-norm of a vector, i.e.,  $\|\mathbf{p}\|_1 = \sum_{i=1}^N |p_i|$ .  $R_{sum}$  is the minimum requirement of the weighted sum-rate, served as the QoS requirement for this battery-saving system.

The problem in (13) has been studied in [70], and it can be converted to a geometric programming (GP) problem involving mean square errors (MSEs), and solved iteratively through downlink-uplink duality [71].

2) *Individual Rate Constraint:* There is a drawback for the joint optimization problem in (10). At the optimal solution, all channel resources, i.e., the transmit power, are allocated to those users with good channel quality so that the corresponding weighted data rates are maximized. Consequently, there will be no or very limited service provided to the rest of users.

To address the inherent unfairness, a variation of the sum-rate maximization problem has been proposed, by adding an additional individual rate constraint for each user. The problem is rewritten as

$$\begin{aligned} & \underset{\mathbf{p}, \mathbf{G}}{\text{maximize}} && \sum_{i=1}^N w_i \log(1 + \text{SINR}_i) \\ & \text{subject to} && \|\mathbf{p}\|_1 \leq P, p_i \geq 0, \\ & && \|\mathbf{g}_i\|_2 = 1, \\ & && \log(1 + \text{SINR}_i) \geq R_i, \forall i \end{aligned} \quad (14)$$

where  $R_i$  denotes the minimum required individual rate for user  $i$ . With a tightened feasible set compared with the one in (10), the optimal weighted sum-rate in (14) is smaller.

In [72], a distributed iterative algorithm for QoS-constrained weighted sum-rate maximization (QCWSRM) problem was proposed based on the alternating direction method of multipliers (ADMM) for the multi-user MIMO beamforming system, after reformulating the problem into an equivalent weighted minimal mean square error (WMMSE) framework.

3) *Dual Problem of the Individual Rate Constraint:* As the dual problem to (14), a joint optimization that minimizes the transmit power is presented, subject to a constraint on the individual rate. The problem is described as follows.

$$\begin{aligned} & \underset{\mathbf{p}, \mathbf{G}}{\text{minimize}} && \|\mathbf{p}\|_1 \\ & \text{subject to} && \log(1 + \text{SINR}_i) \geq R_i, \\ & && p_i \geq 0, \|\mathbf{g}_i\|_2 = 1, \forall i \end{aligned} \quad (15)$$

Here, there is no constraint on the weighted sum-rate of the network. An efficient solution to the problem in (15) has been proposed in [73], with the individual SINR constraint instead of the individual rate constraint. The problem is solved through the following steps.

- 1) The feasibility of (15) is first checked to make sure that the SINR requirements are satisfied. If so, the individual SINR is maximized with an arbitrary total transmit power, which yields a corresponding optimal  $\mathbf{G}$ . This step is similar to the algorithm for solving the max-min SINR problem.
- 2) Then the power allocation  $\mathbf{p}$  is obtained through fixing the individual rate to the lower bound  $R_i$  and with the waveform/beamform  $\mathbf{G}$ . The corresponding optimal power allocation will have a closed form, and the total power consumption will be reduced then.
- 3) Repeat step 1 and 2 with an updated total power constraint  $\|\mathbf{p}\|_1$  until the problem converges or the SINR constraints become infeasible.

*Remark 5:* The disadvantage of obtaining the optimal waveform or beamform from a weighted sum-rate maximization is that the system may fail to achieve a fairness among all users. With the most aggressive objective as to maximize the system throughput, most of resources will be allocated to only a small portion of the users whose channel qualities and thus SINRs are better compared with the others [6].

In the following section, an optimization problem is introduced which achieves a balance, a.k.a., fairness, among users in the network.

### B. Max-Min SINR Maximization

In this part, a joint optimization problem that considers the fairness among users in a multi-user wireless communication system is studied. The QoS criterion for the fairness problem is selected as the received SINR.

In general, in order to achieve fairness in a multi-user downlink system, the max-min SINR problem is proposed, whose objective is to maximize the worst received SINR among all users with a total downlink transmit power constraint. This nonconvex optimization problem is given by

$$\begin{aligned} & \underset{\mathbf{p}, \mathbf{G}}{\text{maximize}} && \min_i \frac{\text{SINR}_i}{\beta_i} \\ & \text{subject to} && \|\mathbf{p}\|_1 \leq P, \quad p_i \geq 0, \\ & && \|\mathbf{g}_i\|_2 = 1, \quad \forall i \end{aligned} \quad (16)$$

where  $\beta_i > 0$  serves as the weight factor to support different priorities or SINR requirements among different users, which is the same as  $w_i$  in (10). Consequently, a higher power will be allocated to a user with a larger  $\beta_i$  to support a higher SINR in the optimal solution. Meanwhile, the weighted SINR  $\frac{\text{SINR}_i}{\beta_i}$  can be viewed as a virtual SINR for user  $i$ , taking into account not only the channel quality but also the individual weighted QoS requirement.

To solve the problem in (16) efficiently, a SINR lower bound  $\gamma$  is introduced as the slack variable and the max-min problem can be rewritten into (17). The joint optimization problem is now aimed at maximizing the lower bound  $\gamma$ .

$$\begin{aligned} & \underset{\mathbf{p}, \mathbf{G}, \gamma}{\text{maximize}} && \gamma \\ & \text{subject to} && \|\mathbf{p}\|_1 \leq P, \quad p_i \geq 0, \\ & && \|\mathbf{g}_i\|_2 = 1, \quad \text{SINR}_i \geq \beta_i \gamma, \quad \forall i \end{aligned} \quad (17)$$

*Remark 6:* The problem in (16) is equivalent to the one in (17) in that the optimum  $\gamma^*$  of (17) is equal to the optimum of the weighted worst SINR in (16), with the same optimal variables  $\mathbf{G}$  and  $\mathbf{p}$  [6], [73].

Subject to the total downlink transmit power constraint, the optimization problem (16) and (17) can be solved by an iterative optimization process as follows.

- 1) First, the downlink problem is converted to an uplink optimization through the downlink-uplink duality [71], with optimal variables  $\mathbf{q}$  and  $\mathbf{S}$ .
- 2) Given an uplink transmit power allocation vector  $\mathbf{q}$ , the optimal uplink waveform/beamforming matrix  $\mathbf{S}$  is the MMSE waveform/beamform defined in Table II.
- 3) Once the waveform/beamforming matrix  $\mathbf{S}$  is fixed, the optimal uplink power allocation vector  $\mathbf{q}$  is obtained through solving a Perron-Frobenius eigen problem.
- 4) Iteratively optimize between step 2 and step 3 until reaching the converging point. Then the optimal waveform/beamform for downlink transmission is  $\mathbf{G}^* = \mathbf{S}^*$ , and the optimal downlink power allocation vector  $\mathbf{p}^*$  has a closed form and can be solved with  $\mathbf{G}^*$ .

*Remark 7:* At the optimum solution, the virtual SINRs  $\frac{\text{SINR}_i}{\beta_i}$  of all users are balanced and the fairness is delivered. In other words, the optimal weighted SINRs for all users in the problem (16) are identical to each other [6], [34].

*Remark 8:* If the max-min problem has an individual power constraint  $\mathbf{p} \preceq \mathbf{p}_{th}$ , then it is first relaxed to have a total power constraint as  $\|\mathbf{p}\|_1 \leq \|\mathbf{p}_{th}\|_1$ . Afterwards, the relaxed problem has the same formulation as in (16) and can be solved iteratively. However, in order to find the optimal power allocation with the corresponding optimal  $\mathbf{G}$ , the total power constraint  $\|\mathbf{p}_{th}\|_1$  should be tightened gradually until the optimal power allocation vector meets the individual power constraint [6].

The detailed solution to the problem in (16) in a MIMO beamforming system is discussed in [34], whereas the details for a wideband waveforming system are studied in [6].

### C. Robustness

All the problems discussed above are based on the assumption that the CSI estimation at the BS is perfect and the channel is stationary and reciprocal. However, in the real world, the CSI estimation is hardly accurate because of quantization errors, temporal and frequency offset in reciprocal channels, as well as continuous fading and fluctuation of channels. Hence, it is reasonable and necessary to take the imperfectness of the CSI estimation into consideration.

In this part, robust transmit strategies against imperfect CSI estimation are discussed with optimal power allocation and waveform/beamform design for a single user downlink system. Aiming at addressing the performance degradation caused by imperfect CSI and improving the robustness of system, the problem is typically formulated as follows.

$$\begin{aligned} & \underset{\mathbf{g}}{\text{maximize}} && \min_{\mathbf{H} \in \mathcal{S}} \text{SNR} \\ & \text{subject to} && \text{Tr}(\mathbf{g}^\dagger \mathbf{g}) \leq P \end{aligned} \quad (18)$$

where SNR denotes the received SNR,  $\mathbf{H}$  is the CSI matrix between the transmitter and the receiver,  $\mathcal{S}$  represents the collection of the possible imperfectness in the CSI estimation,  $P$  gives the constraint on the transmit power, and the function  $\text{Tr}(\cdot)$  is the operation to take the trace of a matrix.

The definition of SNR is different between the MIMO beamforming system and the wideband waveforming system. Assuming the noise has unit variance, the received SNR in a MIMO beamforming system is defined as  $\text{SINR}_{Ea} = \mathbf{g}_l^\dagger \mathbf{H}_{Ea}^\dagger \mathbf{H}_{Ea} \mathbf{g}_l / (\mathbf{g}_E^\dagger \mathbf{H}_{Ea}^\dagger \mathbf{H}_{Ea} \mathbf{g}_E + \mathbf{g}_{AN}^\dagger \mathbf{H}_{Ea}^\dagger \mathbf{H}_{Ea} \mathbf{g}_{AN} + \sigma_{Ea}^2)$ , and the set  $\mathcal{S} = \{\mathbf{\Delta}, \|\mathbf{\Delta}\| \leq \epsilon\}$  is the set for possible errors in the CSI estimation, where  $\epsilon$  denotes the maximal energy of error in the matrix norm [74].

On the other hand, given a zero-mean and unit-variance noise, the received SNR in a wideband waveforming system is given as  $\text{SNR} = |(\mathbf{h} * \mathbf{g})[L]|^2 = \mathbf{g}^\dagger \mathbf{H}^{(\lfloor \frac{L-1}{D} \rfloor + 1)^\dagger} \mathbf{H}^{(\lfloor \frac{L-1}{D} \rfloor + 1)} \mathbf{g}$ . The set  $\mathcal{S}$  in (18) is the collection of convolution matrices  $\mathbf{H}$  defined in (5) that are generated from imperfect CSI estimations.

By introducing a slack variable  $\gamma$ , a variation of the problem in (18) is written as

$$\begin{aligned} & \underset{\mathbf{g}}{\text{maximize}} && \gamma \\ & \text{subject to} && \min_{\mathbf{H} \in \mathcal{S}} \text{SNR} \geq \gamma, \quad \text{Tr}(\mathbf{g}^\dagger \mathbf{g}) \leq P \end{aligned} \quad (19)$$

TABLE III  
WAVEFORM/BEAMFORM DESIGN FOR OPTIMAL RESOURCE ALLOCATION

	Sum-Rate Maximization	Max-Min SINR	Robustness
<b>Problem Formulation</b>	$\begin{aligned} & \text{maximize}_{\mathbf{p}, \mathbf{G}} \sum_{i=1}^N w_i \log(1 + \text{SINR}_i) \\ & \text{subject to } \ \mathbf{p}\ _1 \leq P, p_i \geq 0, \\ & \ \mathbf{g}_i\ _2 = 1, \forall i \end{aligned}$	$\begin{aligned} & \text{maximize}_{\mathbf{p}, \mathbf{G}} \min_i \frac{\text{SINR}_i}{\beta_i} \\ & \text{subject to } \ \mathbf{p}\ _1 \leq P, p_i \geq 0, \\ & \ \mathbf{g}_i\ _2 = 1, \forall i \end{aligned}$	$\begin{aligned} & \text{maximize}_{\mathbf{g}} \min_{\mathbf{H} \in \mathcal{S}} \text{SNR} \\ & \text{subject to } \text{Tr}(\mathbf{g}^\dagger \mathbf{g}) \leq P \end{aligned}$
<b>Solution</b>	MMSE waveforming Power waterfilling	MMSE waveforming Perron-Frobenius eigen problem	Semi-definite programming (SDP)

where  $\gamma$  serves as the lower bound on the worst received SNR among all possible imperfect CSI matrices.

After rewritten into the form of (19), the joint optimization problem in (18) can be addressed after being relaxed relaxing into a semi-definite programming (SDP) problem, which can be solved efficiently.

Moreover, with the objective of minimizing the total transmit power under a minimum individual SNR requirement, the dual problem to (18) is proposed as follows.

$$\begin{aligned} & \text{minimize}_{\mathbf{g}} \text{Tr}(\mathbf{g}^\dagger \mathbf{g}) \\ & \text{subject to } \min_{\mathbf{H} \in \mathcal{S}} \text{SNR} \geq \gamma \end{aligned} \quad (20)$$

where  $\gamma$  is no longer an optimal variable.

The optimal wideband waveforming for robustness has been proposed for indoor locationing applications to adjust the size of the TR resonating ball and thus the locationing resolution, considering the back-off factor  $D$  is much larger than the delay spread to eliminate ISI [75]. Due to the large delay spread in the wideband system, the ISI is significant and may degrade the received signal quality measured by the received SINR. Hence, it is worthwhile to evaluate and optimize the robustness in a wideband waveforming system, which is discussed in the following.

1) *Robustness of a Single-User Wideband Waveforming System:* To begin with, considering a single-user wideband communication system, the received SINR is defined in (12) with only ISI contributes as the interference. Then, the robustness optimization problem for the single-user wideband waveforming system becomes a max-min SINR problem and is given by

$$\begin{aligned} & \text{maximize}_{\mathbf{g}} \min_{\mathbf{H} \in \mathcal{S}} \text{SINR} \\ & \text{subject to } \text{Tr}(\mathbf{g}^\dagger \mathbf{g}) \leq P \end{aligned} \quad (21)$$

where  $\mathcal{S}$  is the collection of convolution matrices generated by imperfect CSI estimations.

2) *Robustness of a Multi-User Wideband Broadcasting Waveforming System:* In a multi-user broadcasting system, since the BS transmits the same signal to all users with the same power, there is no IUI and users share the same waveform  $\mathbf{g}$ . Hence, the received SINR for user  $j$  is rewritten as follows.

Given the definition of SINR in (12), the robustness problem in multi-user broadcasting system is then formulated as

$$\begin{aligned} & \text{maximize}_{\mathbf{g}} \min_{\mathbf{H}_j \in \mathcal{S}_{j,j}} \text{SINR}_j \\ & \text{subject to } \text{Tr}(\mathbf{g}^\dagger \mathbf{g}) \leq P \end{aligned} \quad (22)$$

where  $\mathcal{S}_j$  is the set of channel matrices from all possible imperfect CSI estimations of user  $j$ .

3) *Robustness of a Multi-User Wideband Multicasting Waveforming System:* In this kind of system, both ISI and IUI exist, due to the fact that the transmitted signal is the combination of different messages with different waveforms through the same wireless medium. Consequently, the received SINR for user  $j$  is exactly same as in (12). Then, the robustness problem becomes a joint optimization problem of the waveform  $\mathbf{G}$  and the power  $\mathbf{p}$  to maximize the worst SINR among all users against the imperfect CSI estimation. It can be rewritten as

$$\begin{aligned} & \text{maximize}_{\mathbf{G}} \min_{\mathbf{H}_j \in \mathcal{S}_{j,j}} \text{SINR}_j \\ & \text{subject to } \text{Tr}(\mathbf{G}^\dagger \mathbf{G}) \leq P \end{aligned} \quad (23)$$

where  $\mathbf{G}$  is the waveforming matrix for all users and the problem in (23) has a similar form to the max-min optimization in (16).

*Remark 9:* The three aforementioned robustness problem for wideband waveforming systems has a similar problem formulation as the max-min optimization one in (16) in Section IV-B. However, here it adopts a unified weight factor  $\beta_i = 1, \forall i$  and an additional set of possible SINRs associated with different channels for the same user. Nevertheless, same algorithms can be applied to efficiently solve the aforementioned robustness problem with SINR as the criterion.

Table III summarizes the optimization problems studied in this section.

## V. WIRELESS POWERED COMMUNICATION

Traditional wireless communications are primarily constrained by the limited accessibility of spectrum resources [76], [77]. Nevertheless, as proposed for the next generation wireless communication system, the network will be moved to a higher frequency band with a larger bandwidth, leading to ample spectrum resources. However, due to the explosive growth of wireless data services and the demand of a significantly high rate in data transmission,

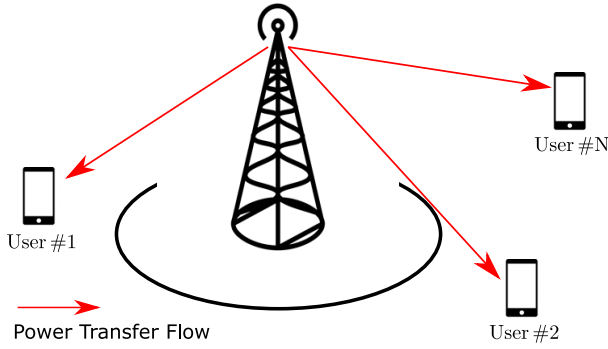


Fig. 8. A WPT system.

wireless devices are subject to limited energy resources, such that convenient and perpetual energy supplies are indispensable. In this section, the comparison between the MIMO beamforming and the wideband waveforming in the wireless powered communication system is discussed.

The wireless powered communication system can operate in three different modes. The first is the WPT system where the receiver only receives power without decoding the message sent from the transmitter. Moreover, the wireless powered communication can operate in a way such that the power is transferred wirelessly during the downlink whereas information is sent in the uplink with the energy harvested from the downlink transmission. The third operating mode is called the simultaneous wireless information and power transfer (SWIPT) which simultaneously supports the transmission of both the energy and the information during downlink but under a constraint on the power and spectrum consumption [35]–[38]. The detailed discussion is as follows.

#### A. Wireless Power Transfer System

To begin with, the WPT system is studied in this part with the objective to pursue a maximal reception power under a constraint on the total transmit power. A system diagram is shown in Fig. 8. The mathematical formulation of the WPT problem becomes

$$\begin{aligned} & \underset{\mathbf{g}}{\text{maximize}} && E\left[\|\mathbf{y}\|_2^2\right] \\ & \text{subject to} && \text{Tr}(\mathbf{g}^\dagger \mathbf{g}) \leq P \end{aligned} \quad (24)$$

where  $\mathbf{y}$  denotes the received signal,  $\mathbf{g}$  is the energy waveform or beamform for WPT, and  $P$  is the maximum total transmit power. The definition of the received energy  $\|\mathbf{y}\|_2^2$  is different in the MIMO beamforming system and the wideband waveforming system. In the MIMO beamforming system, it is defined as  $\|\mathbf{y}\|_2^2 = \mathbf{g}^\dagger \mathbf{H}^\dagger \mathbf{H} \mathbf{g}$ , where  $\mathbf{H}$  is the MIMO channel matrix [35].

On the other hand, in the wideband waveforming system, the definition of  $\|\mathbf{y}\|_2^2$  is given in [24] as  $\|\mathbf{y}\|_2^2 = |(\mathbf{h} * \mathbf{g})[L]|^2 = \mathbf{g}^\dagger \mathbf{H}^{(\lfloor \frac{L-1}{D} \rfloor + 1)^\dagger} \mathbf{H}^{(\lfloor \frac{L-1}{D} \rfloor + 1)} \mathbf{g}$ .

According to the definition of  $\|\mathbf{y}\|_2^2$ , it is easy to find out that the optimal energy waveform or beamform for the WPT

problem in (24) is the principal eigenvector of channel covariance matrix, which is  $\mathbf{H}^\dagger \mathbf{H}$  for a MIMO WPT system and  $\mathbf{H}^{(\lfloor \frac{L-1}{D} \rfloor + 1)^\dagger} \mathbf{H}^{(\lfloor \frac{L-1}{D} \rfloor + 1)}$  for a wideband WPT system.

Furthermore, the single-tone waveforming/beamforming has been proposed as a simple but sub-optimal solution for WPT, where all the power is allocated on the most efficient frequency component of the channel [24]. Considering the fact that the optimal energy waveform or beamform maximizes the average received power in time domain, it is superior to any other schemes. Hence, the harvested energy by means of the single-tone waveform or beamform can serve as a performance lower bound of the optimal energy waveform or beamform.

To achieve the single-tone waveforming in the wideband system, the following steps are went through:

- 1) The user channel  $\mathbf{h}$  is first converted into the frequency domain channel through the Discrete Fourier transform (DFT) operation  $\text{DFT}(\mathbf{h})$ .
- 2) Afterwards, the principal component  $\delta$  is discovered from  $\delta = \text{argmax}_k \text{DFT}(\mathbf{h})[k]$ , where  $k$  is the index of frequency component.
- 3) Finally, the single-tone waveform  $\mathbf{g}$  is obtained by the inverse-DFT of  $\delta$ ,  $\text{IDFT}(\delta)$ .

However, in order to find the single-tone beamform for the MIMO system, a 2-D DFT is required because the channel  $\mathbf{H}$  is a matrix.

*Remark 10:* For periodical signals, the single-tone waveform is the same as the optimal energy waveform obtained from (24), because the DFT matrix becomes a singular matrix of the channel covariance matrix [24].

#### B. Simultaneous Wireless Information and Power Transfer

In this part, the SWIPT system is studied where the WPT and wireless communications are conducted simultaneously. The performance trade-off between the delivered energy and the information capacity for the SWIPT system has been studied in [78] and [79]. Huang and Larsson [80] has investigated a broadband SWIPT system where OFDM and beamform design are deployed to create parallel subchannels to simplify resource allocation. In the following, two major kinds of optimization problems that consider the energy-information trade-off in SWIPT are introduced.

1) *Interference as Energy:* The first formulation is a joint information and energy waveform/beamform design problem, which treats the interference from information delivery as the transmitted energy. An example of system diagram is shown in Fig. 9a. It is designed to maximize the weighted sum-power delivered to all receivers subject to individual SINR constraints [36] as

$$\begin{aligned} & \underset{\mathbf{g}_E, \mathbf{g}_I}{\text{maximize}} && E\left[\|\mathbf{y}_E\|_2^2\right] + E\left[\|\mathbf{y}_I\|_2^2\right] \\ & \text{subject to} && \text{Tr}(\mathbf{g}_E^\dagger \mathbf{g}_E) + \text{Tr}(\mathbf{g}_I^\dagger \mathbf{g}_I) \leq P, \\ & && \text{SINR}_I \geq \gamma \end{aligned} \quad (25)$$

where  $\mathbf{g}_E$  is the waveform or beamform for power transfer,  $\mathbf{g}_I$  represents the waveform or beamform for information delivery,  $\mathbf{y}_E$  is the power signal received at the power receiver,  $\mathbf{y}_I$  is the information signal received at the power receiver, and  $\text{SINR}_I$

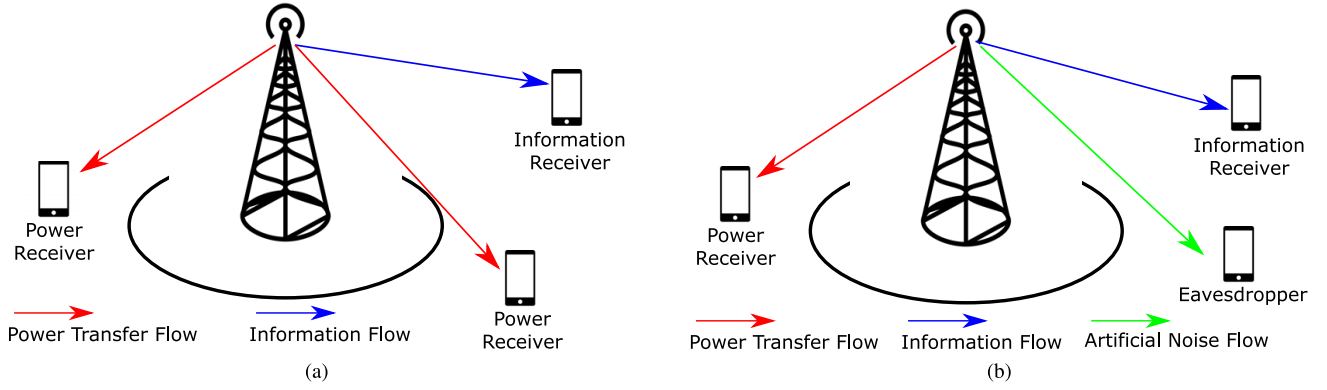


Fig. 9. Examples of SWIPT. (a) Interference as energy. (b) Interference as security.

represents the received SINR of the information signal at the information receiver.

In the MIMO beamforming system, the received energy at the energy receiver contains  $\|\mathbf{y}_E\|_2^2 = \mathbf{g}_E^\dagger \mathbf{H}_E^\dagger \mathbf{H}_E \mathbf{g}_E$  and  $\|\mathbf{y}_I\|_2^2 = \mathbf{g}_I^\dagger \mathbf{H}_E^\dagger \mathbf{H}_E \mathbf{g}_I$ , where  $\mathbf{H}_E$  is the channel matrix between the BS and the power receiver and  $\mathbf{H}_I$  is the channel matrix between the BS and the information receiver. The received SINR of the information signal at the information receiver,  $\text{SINR}_I$ , is defined in (11).

On the other hand, in a wideband waveforming system, the SINR of the information signal at the information receiver follows the definition in (12), with  $\mathbf{g}_I$  and  $\mathbf{H}_I$  as the intended waveform and channel matrix. Moreover, considering the existence of ISI, the definitions of received energy at the power receiver from the energy waveform is different, i.e.,  $\|\mathbf{y}_E\|_2^2 = |(\mathbf{h}_E * \mathbf{g}_E)[L]|^2 = \mathbf{g}_E^\dagger \mathbf{H}_E^{(\lfloor \frac{L-1}{D} \rfloor + 1)^\dagger} \mathbf{H}_E^{(\lfloor \frac{L-1}{D} \rfloor + 1)} \mathbf{g}_E$ , compared with the definition in the MIMO beamforming system.

The joint information and power transfer waveform/beamform optimization with the problem formulation in (25) is a non-convex quadratically constrained quadratic program (QCQP). The problem can be addressed in the following steps.

- 1) The first is to check the feasibility of (25). In particular, the problem is feasible when the SINR constraint for information users are achievable without considering energy users.
- 2) If the problem is feasible, then a semi-definite relaxation (SDR) is applied to convert the non-convex QCQP problem into a semi-definite program (SDP) which can be solved efficiently.

For a MIMO SWIPT system, it has been proved that for the problem in (25), under the condition of independently distributed user channels, there is no need to design dedicated energy beamforming vector. The optimal transmission strategy is to adjust the weights and power allocation of only the information beamforming to maximize the sum-power delivered [36]. Moreover, since the energy waveform/beamform is not for information transmission, an interference pre-cancellation might be adopted at the information receiver, to further improve the received SINR.

An alternative formulation of waveform/beamform design which considers the information-energy trade-off is to

maximize the information rate under the constraint of the delivered power, as the dual problem to the aforementioned one in (25). The mathematical formulation of the dual problem can be written as

$$\begin{aligned}
 & \underset{\mathbf{g}_E, \mathbf{g}_I}{\text{maximize}} && \log(1 + \text{SINR}_I) \\
 & \text{subject to} && \text{Tr}(\mathbf{g}_E^\dagger \mathbf{g}_E) + \text{Tr}(\mathbf{g}_I^\dagger \mathbf{g}_I) \leq P, \\
 & && E[\|\mathbf{y}_E\|_2^2] + E[\|\mathbf{y}_I\|_2^2] \geq P_{th} \quad (26)
 \end{aligned}$$

where  $\text{SINR}_I$  is the received SINR at the information receiver,  $\mathbf{y}_I$  and  $\mathbf{y}_E$  are the received signal at the energy receiver from the information transmitter and the energy transmitter, respectively.  $P_{th}$  is the minimum required power delivered to the energy transmitter.

2) *Interference As Security*: In [41] and [81], by using the energy beamform as a secrecy enhancement tool, the resource allocation algorithm is designed for secure communication in MIMO beamforming systems with concurrent wireless information and power transfer. This formulation, named as interference-as-security, was proposed to minimize the transmit power, by leveraging both the artificial noise and energy beamforms to facilitate an efficient energy transfer and ensure the communication security. The system demonstration is depicted in Fig. 9b, and a generalized and simplified mathematical problem formulation is written as follows.

$$\begin{aligned}
 & \underset{\mathbf{g}_E, \mathbf{g}_I, \mathbf{g}_{AN}}{\text{maximize}} && \log(1 + \text{SINR}_I) - R \\
 & \text{subject to} && \text{Tr}(\mathbf{g}_E^\dagger \mathbf{g}_E) + \text{Tr}(\mathbf{g}_I^\dagger \mathbf{g}_I) + \text{Tr}(\mathbf{g}_{AN}^\dagger \mathbf{g}_{AN}) \leq P, \\
 & && \max\{\log(1 + \text{SINR}_E), \log(1 + \text{SINR}_{Ea})\} = R, \\
 & && \text{SINR}_I \geq R_I, \\
 & && \|\mathbf{y}_I\|_2^2 + \|\mathbf{y}_E\|_2^2 + \|\mathbf{y}_{AN}\|_2^2 \geq P_{th} \quad (27)
 \end{aligned}$$

where  $\text{SINR}_I$ ,  $\text{SINR}_E$ ,  $\text{SINR}_{Ea}$  are the received SINR at the information receiver, the energy receiver, and the eavesdropper, respectively.  $\mathbf{g}_E$ ,  $\mathbf{g}_I$  and  $\mathbf{g}_{AN}$  are the waveforming/beamforming vector for the energy transmission, information transmission and artificial noise.  $\|\mathbf{y}_I\|_2^2 + \|\mathbf{y}_E\|_2^2 + \|\mathbf{y}_{AN}\|_2^2$  denotes the total power delivered at the energy receiver, which can be decomposed into the energy from the information transmission, the energy transfer and the artificial noise transmission, correspondingly.

TABLE IV  
WAVEFORM/BEAMFORM DESIGN IN WIRELESS POWERED COMMUNICATIONS

	WPT	SWIPT - Interference as Energy	SWIPT - Interference as Security
<b>Problem Formulation</b>	$\max_{\mathbf{g}} E \left[ \ \mathbf{y}\ _2^2 \right]$	$\max_{\mathbf{g}_E, \mathbf{g}_I} E \left[ \ \mathbf{y}_E\ _2^2 \right] + E \left[ \ \mathbf{y}_I\ _2^2 \right]$	$\max_{\substack{\mathbf{g}_E, \mathbf{g}_I, \\ \mathbf{g}_{AN}}} \log(1 + \text{SINR}_I) - R$
	s.t. $\text{Tr}(\mathbf{g}^\dagger \mathbf{g}) \leq P$	s.t. $\text{Tr}(\mathbf{g}_E^\dagger \mathbf{g}_E) + \text{Tr}(\mathbf{g}_I^\dagger \mathbf{g}_I) \leq P,$ $\text{SINR}_I \geq \gamma$	s.t. $\text{Tr}(\mathbf{g}_E^\dagger \mathbf{g}_E) + \text{Tr}(\mathbf{g}_I^\dagger \mathbf{g}_I) + \text{Tr}(\mathbf{g}_{AN}^\dagger \mathbf{g}_{AN}) \leq P,$ $\max\{\log(1 + \text{SINR}_E), \log(1 + \text{SINR}_{Ea})\} = R,$ $\text{SINR}_I \geq R_I,$ $\ \mathbf{y}_I\ _2^2 + \ \mathbf{y}_E\ _2^2 + \ \mathbf{y}_{AN}\ _2^2 \geq P_{th}$
<b>Solution</b>	Principal eigenvector of channel covariance	SDP after semi-definite relaxations (SDRs)	SDP after SDRs

In the MIMO beamforming system, given the prior knowledge of energy waveform for interference pre-cancellation at the intended information receiver, the definitions of SINRs in (27) are different. For  $\text{SINR}_I$  and  $\text{SINR}_E$ , interference only comes from IUI of waveform  $\mathbf{g}_{AN}$ , i.e.,  $\text{SINR}_I = \mathbf{g}_I^\dagger \mathbf{H}_I^\dagger \mathbf{H}_I \mathbf{g}_I / (\mathbf{g}_{AN}^\dagger \mathbf{H}_I^\dagger \mathbf{H}_I \mathbf{g}_{AN} + \sigma_I^2)$  and  $\text{SINR}_E = \mathbf{g}_I^\dagger \mathbf{H}_E^\dagger \mathbf{H}_E \mathbf{g}_I / (\mathbf{g}_{AN}^\dagger \mathbf{H}_E^\dagger \mathbf{H}_E \mathbf{g}_{AN} + \sigma_I^2)$ . On the other hand, the received SINR at the eavesdropper follows the definition in (11) and both  $\mathbf{g}_{AN}$  and  $\mathbf{g}_E$  contributes to the IUI, i.e.,  $\text{SINR}_{Ea} = \mathbf{g}_I^\dagger \mathbf{H}_{Ea}^\dagger \mathbf{H}_{Ea} \mathbf{g}_I / (\mathbf{g}_E^\dagger \mathbf{H}_{Ea}^\dagger \mathbf{H}_{Ea} \mathbf{g}_E + \mathbf{g}_{AN}^\dagger \mathbf{H}_{Ea}^\dagger \mathbf{H}_{Ea} \mathbf{g}_{AN} + \sigma_{Ea}^2)$ .  $\mathbf{H}_I$ ,  $\mathbf{H}_E$ ,  $\mathbf{H}_{Ea}$  represent the channel from the transmitter to the information receiver, the energy receiver and the eavesdropper, respectively.  $\sigma_I^2$ ,  $\sigma_E^2$  and  $\sigma_{AE}^2$  are the noise variance at the corresponding receiver side. The total power delivered is given as  $\|\mathbf{y}_I\|_2^2 + \|\mathbf{y}_E\|_2^2 + \|\mathbf{y}_{AN}\|_2^2 = \mathbf{g}_I^\dagger \mathbf{H}_E^\dagger \mathbf{H}_E \mathbf{g}_I + \mathbf{g}_E^\dagger \mathbf{H}_E^\dagger \mathbf{H}_E \mathbf{g}_E + \mathbf{g}_{AN}^\dagger \mathbf{H}_E^\dagger \mathbf{H}_E \mathbf{g}_{AN}$ .

The solution of this problem has been studied in [41], which was solved through a series of relaxations including SDRs. Then a suboptimal resource allocation scheme with low computational complexity was designed to support both WPT and secured communication.

However, the mathematical details for the problem in (27) are more complicated in the wideband waveforming system, and the related study is still open.

Waveform design for problems in WPT and SWIPT studied in this section is summarized in Table IV.

## VI. SECURED COMMUNICATIONS

In wireless communications, the broadcasting nature of wireless media grants access to the transmitted information not only for intended receivers but also for eavesdroppers. Hence, security becomes a fundamental and critical problem to the wireless communication system, due to the openness of wireless media that makes it vulnerable to potential eavesdropping.

Recently, a plenty of research has been conducted to the information-theoretic physical (PHY) layer security which exploits the physical characteristics of the wireless fading channel to offer a perfect secrecy [41]. The artificial noise (AN) has been proposed as an effective method to impair

the received signals at the eavesdroppers by utilizing the extra degrees of freedom offered by multiple antennas in the MIMO system [39]–[42].

In a MIMO beamforming system with the presence of the artificial noise, the system model is discussed in [40] and [42] and the details are as follows. Firstly, the transmit signal is defined as

$$\mathbf{s} = \mathbf{G}^d \mathbf{x} + \mathbf{G}^{AN} \mathbf{a} \quad (28)$$

where  $\mathbf{G}^d$  is the data beamform and  $\mathbf{G}^{AN}$  is the AN beamforming vector.  $\mathbf{x}$  denotes the information signal and  $\mathbf{a}$  represents the AN signal.

The received signal can be written and decoupled into two groups, one for the intended receiver Bob and the other for the eavesdropper Eve. The received signal for the intended receiver Bob can be written as  $\mathbf{y}_b = \mathbf{H}_b \mathbf{s} + \mathbf{n}_b = \mathbf{H}_b \mathbf{G}^d \mathbf{x} + \mathbf{H}_b \mathbf{G}^{AN} \mathbf{a} + \mathbf{n}_b$ , and the received signal for eavesdropper Eve is given by  $\mathbf{y}_e = \mathbf{H}_e \mathbf{s} + \mathbf{n}_e = \mathbf{H}_e \mathbf{G}^d \mathbf{x} + \mathbf{H}_e \mathbf{G}^{AN} \mathbf{a} + \mathbf{n}_e$ .

Here,  $\mathbf{H}_b$  is the channel between the transmitter and Bob,  $\mathbf{n}_b$  is the noise at the receiver side of Bob,  $\mathbf{H}_e$  is the channel between the transmitter and Eve, and  $\mathbf{n}_e$  is the noise for Eve. Moreover,  $\mathbf{H}_b \mathbf{G}^{AN} \mathbf{a} = \mathbf{0}$ , which means the AN precoder  $\mathbf{G}^{AN}$  is in the null space of Bob's channel  $\mathbf{H}_b$ . Given the fact that  $\mathbf{H}_b$  is of full row rank, the precoder, i.e., the AN beamform  $\mathbf{G}_{AN}$  is defined as follows [40].

$$\mathbf{G}^{AN} = \mathbb{I} - \mathbf{H}_b^\dagger (\mathbf{H}_b \mathbf{H}_b^\dagger)^{-1} \mathbf{H}_b \quad (29)$$

The optimization problem for the MIMO beamforming with AN is studied in [42], where the objective is maximize the secrecy capacity, subject to a SINR and a power constraint. The performance, measured by achievable ergodic secrecy rates are analyzed with four different data beamforms and three different AN beamforms.

In the wideband waveforming system, each tap in the CSI is viewed as a virtual antenna and the antenna diversity is achieved by multiple virtual antennas, which enabling the AN for the secrecy improvement. According to (4), the received signal at the intended information receiver, Bob, can be rewritten as  $\mathbf{y}_b = \mathbf{H}_b \mathbf{g}_d \mathbf{x} + \mathbf{H}_b \mathbf{g}_{AN} \mathbf{a} + \mathbf{n}_b$ , where  $\mathbf{H}_b$  is the channel matrix between the BS and Bob, as defined in (5).  $\mathbf{g}_d$  and  $\mathbf{g}_{AN}$

represent the data waveform and the AN waveform, respectively.  $\mathbf{x}$  is the transmit information signal and  $\mathbf{a}$  denotes the AN signal.  $\mathbf{n}_b$  is a white Gaussian noise at the receiver.

Similarly, the received signal at the eavesdropper is given by  $\mathbf{y}_e = \mathbf{H}_e \mathbf{g}_d * \mathbf{x} + \mathbf{H}_e \mathbf{g}_{AN} * \mathbf{a} + \mathbf{n}_e$ , where  $\mathbf{H}_b$  is the channel matrix between the BS and eavesdropper and  $\mathbf{n}_e$  is the received white Gaussian noise.

Considering the quality of received signal at the intended information receiver, we must have the waveforming vector  $\mathbf{g}_{AN}$  lie in the null space of the channel matrix  $\mathbf{H}_b$ , i.e.,  $\mathbf{H}_b \mathbf{g}_{AN} = \mathbf{0}$ . Moreover, in order to have at least one solution for  $\mathbf{g}_{AN}$  feasible,  $\mathbf{H}_b$  must have a full row rank. The channel matrix  $\mathbf{H}_b$  as defined in (5), has a dimension of  $N \left( 2 \lfloor \frac{L-1}{D} \rfloor + 1 \right) \times L$ . Hence,  $\mathbf{H}_b$  is of full row rank if and only if  $L \leq \frac{2N-DN}{2N-D}$  when  $D < 2N$ , or  $L \geq \frac{DN-2N}{D-2N}$  when  $D > 2N$ . If  $D = 2N$ , then only  $N = 1$  yields a full row rank matrix. The related study for wideband waveforming in secured communication systems with AN transmission is still open.

## VII. CONCLUSION

By leveraging multipaths in the nature, waveforming is proposed as a prominent technique for the wideband system to exploit spatial diversity. Waveforming harvests large degrees of freedom, by treating each multipath component in a multipath channel as a virtual antenna and weighing and combining information coherently. Hence, the wideband waveforming becomes an economic and promising solution to future communication systems which support low-cost low-complexity implementation and high data rate wireless services. In this paper, we summarize the novel wideband waveforming system, and compare it with the conventional narrowband MIMO beamforming system where high degrees of freedom are achieved by transmitting with multiple antennas. System models and related optimization problems on resource allocation, powered wireless communications and secured communications are studied in detail.

## REFERENCES

- [1] B. Wang, Y. Wu, F. Han, Y.-H. Yang, and K. J. R. Liu, "Green wireless communications: A time-reversal paradigm," *IEEE J. Sel. Areas Commun.*, vol. 29, no. 8, pp. 1698–1710, Sep. 2011.
- [2] Y.-H. Yang, B. Wang, W. S. Lin, and K. J. R. Liu, "Near-optimal waveform design for sum rate optimization in time-reversal multiuser downlink systems," *IEEE Trans. Wireless Commun.*, vol. 12, no. 1, pp. 346–357, Jan. 2013.
- [3] F. Han and K. J. R. Liu, "A multiuser TRDMA uplink system with 2D parallel interference cancellation," *IEEE Trans. Commun.*, vol. 62, no. 3, pp. 1011–1022, Mar. 2014.
- [4] E. Yoon, S.-Y. Kim, and U. Yun, "A time-reversal-based transmission using pre-distortion for intersymbol interference alignment," *IEEE Trans. Commun.*, vol. 63, no. 2, pp. 455–465, Feb. 2015.
- [5] Y.-H. Yang and K. J. R. Liu, "Waveform design with interference pre-cancellation beyond time-reversal systems," *IEEE Trans. Wireless Commun.*, vol. 15, no. 5, pp. 3643–3654, May 2016.
- [6] Q. Xu, Y. Chen, and K. J. R. Liu, "Combating strong-weak spatial-temporal resonances in time-reversal uplinks," *IEEE Trans. Wireless Commun.*, vol. 15, no. 1, pp. 568–580, Jan. 2016.
- [7] M. Fink, C. Prada, F. Wu, and D. Cassereau, "Self focusing in inhomogeneous media with time reversal acoustic mirrors," in *Proc. IEEE Ultrason. Symp.*, Montreal, QC, Canada, 1989, pp. 681–686.
- [8] M. Fink, "Time reversal of ultrasonic fields. I. Basic principles," *IEEE Trans. Ultrason., Ferroelectr., Freq. Control*, vol. 39, no. 5, pp. 555–566, Sep. 1992.
- [9] A. Derode, P. Roux, and M. Fink, "Robust acoustic time reversal with high-order multiple scattering," *Phys. Rev. Lett.*, vol. 75, no. 23, pp. 4206–4209, 1995.
- [10] H. C. Song, W. Kuperman, W. S. Hodgkiss, T. Akal, and C. Ferla, "Iterative time reversal in the ocean," *J. Acoust. Soc. Amer.*, vol. 105, no. 6, pp. 3176–3184, 1999.
- [11] H. T. Nguyen, I. Z. Kovcs, and P. C. F. Eggers, "A time reversal transmission approach for multiuser UWB communications," *IEEE Trans. Antennas Propag.*, vol. 54, no. 11, pp. 3216–3224, Nov. 2006.
- [12] R. C. Qiu, C. Zhou, N. Guo, and J. Q. Zhang, "Time reversal with MISO for ultra-wideband communications: Experimental results," in *Proc. IEEE Radio Wireless Symp.*, San Diego, CA, USA, Jan. 2006, pp. 499–502.
- [13] R. L. D. L. Neto, A. M. Hayar, and M. Debbah, "Channel division multiple access based on high UWB channel temporal resolution," in *Proc. IEEE Veh. Technol. Conf.*, Montreal, QC, Canada, Sep. 2006, pp. 1–5.
- [14] N. Guo, B. M. Sadler, and R. C. Qiu, "Reduced-complexity UWB time-reversal techniques and experimental results," *IEEE Trans. Wireless Commun.*, vol. 6, no. 12, pp. 4221–4226, Dec. 2007.
- [15] A. Khaleghi, G. E. Zein, and I. H. Naqvi, "Demonstration of time-reversal in indoor ultra-wideband communication: Time domain measurement," in *Proc. 4th Int. Symp. Wireless Commun. Syst.*, Trondheim, Norway, Oct. 2007, pp. 465–468.
- [16] M.-A. Bouzigues, I. Siaud, M. Helard, and A. M. Ulmer-Moll, "Turn back the clock: Time reversal for green radio communications," *IEEE Veh. Technol. Mag.*, vol. 8, no. 1, pp. 49–56, Mar. 2013.
- [17] H. T. Nguyen, J. B. Andersen, and G. F. Pedersen, "The potential use of time reversal techniques in multiple element antenna systems," *IEEE Commun. Lett.*, vol. 9, no. 1, pp. 40–42, Jan. 2005.
- [18] Y. Jin, Y. Jiang, and J. M. F. Moura, "Multiple antenna time reversal transmission in ultra-wideband communications," in *Proc. IEEE GLOBECOM Glob. Telecommun. Conf.*, Washington, DC, USA, Nov. 2007, pp. 3029–3033.
- [19] C. Zhou, N. Guo, B. M. Sadler, and R. C. Qiu, "Performance study on time reversed impulse MIMO for UWB communications based on measured spatial UWB channels," in *Proc. IEEE Mil. Commun. Conf. MILCOM*, Orlando, FL, USA, Oct. 2007, pp. 1–6.
- [20] A. Pitarokoilis, S. K. Mohammed, and E. G. Larsson, "Uplink performance of time-reversal MRC in massive MIMO systems subject to phase noise," *IEEE Trans. Wireless Commun.*, vol. 14, no. 2, pp. 711–723, Feb. 2015.
- [21] M. Maaz, M. Helard, P. Mary, and M. Liu, "Performance analysis of time-reversal based precoding schemes in MISO-OFDM systems," in *Proc. IEEE 81st Veh. Technol. Conf. (VTC Spring)*, Glasgow, U.K., May 2015, pp. 1–6.
- [22] F. Han, Y.-H. Yang, B. Wang, Y. Wu, and K. J. R. Liu, "Time-reversal division multiple access over multi-path channels," *IEEE Trans. Commun.*, vol. 60, no. 7, pp. 1953–1965, Jul. 2012.
- [23] Y. Chen *et al.*, "Time-reversal wireless paradigm for green Internet of Things: An overview," *IEEE Internet Things J.*, vol. 1, no. 1, pp. 81–98, Feb. 2014.
- [24] M.-L. Ku, Y. Han, H.-Q. Lai, Y. Chen, and K. J. R. Liu, "Power waveforming: Wireless power transfer beyond time reversal," *IEEE Trans. Signal Process.*, vol. 64, no. 22, pp. 5819–5834, Nov. 2016.
- [25] D. Gesbert, M. Shafi, D.-S. Shiu, P. J. Smith, and A. Naguib, "From theory to practice: An overview of MIMO space-time coded wireless systems," *IEEE J. Sel. Areas Commun.*, vol. 21, no. 3, pp. 281–302, Apr. 2003.
- [26] L. Zheng and D. N. C. Tse, "Diversity and multiplexing: A fundamental tradeoff in multiple-antenna channels," *IEEE Trans. Inf. Theory*, vol. 49, no. 5, pp. 1073–1096, May 2003.
- [27] R. W. Heath and A. J. Paulraj, "Switching between diversity and multiplexing in MIMO systems," *IEEE Trans. Commun.*, vol. 53, no. 6, pp. 962–968, Jun. 2005.
- [28] H. Q. Ngo, E. G. Larsson, and T. L. Marzetta, "Energy and spectral efficiency of very large multiuser MIMO systems," *IEEE Trans. Commun.*, vol. 61, no. 4, pp. 1436–1449, Apr. 2013.
- [29] J. G. Andrews *et al.*, "What will 5G be?" *IEEE J. Sel. Areas Commun.*, vol. 32, no. 6, pp. 1065–1082, Jun. 2014.
- [30] F. Boccardi, R. W. Heath, A. Lozano, T. L. Marzetta, and P. Popovski, "Five disruptive technology directions for 5G," *IEEE Commun. Mag.*, vol. 52, no. 2, pp. 74–80, Feb. 2014.
- [31] Y. Han, Y. Chen, B. Wang, and K. J. R. Liu, "Time-reversal massive multipath effect: A single-antenna 'massive MIMO' solution," *IEEE Trans. Commun.*, vol. 64, no. 8, pp. 3382–3394, Aug. 2016.
- [32] B. D. V. Veen and K. M. Buckley, "Beamforming: A versatile approach to spatial filtering," *IEEE ASSP Mag.*, vol. 5, no. 2, pp. 4–24, Apr. 1988.

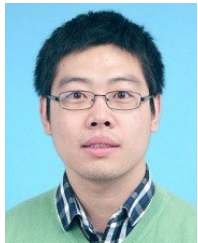
- [33] D. P. Palomar, J. M. Cioffi, and M. A. Lagunas, "Joint Tx-Rx beamforming design for multicarrier MIMO channels: A unified framework for convex optimization," *IEEE Trans. Signal Process.*, vol. 51, no. 9, pp. 2381–2401, Sep. 2003.
- [34] C. W. Tan, M. Chiang, and R. Srikant, "Maximizing sum rate and minimizing MSE on multiuser downlink: Optimality, fast algorithms and equivalence via max-min SINR," *IEEE Trans. Signal Process.*, vol. 59, no. 12, pp. 6127–6143, Dec. 2011.
- [35] R. Zhang and C. K. Ho, "MIMO broadcasting for simultaneous wireless information and power transfer," *IEEE Trans. Wireless Commun.*, vol. 12, no. 5, pp. 1989–2001, May 2013.
- [36] J. Xu, L. Liu, and R. Zhang, "Multiuser MISO beamforming for simultaneous wireless information and power transfer," *IEEE Trans. Signal Process.*, vol. 62, no. 18, pp. 4798–4810, Sep. 2014.
- [37] Q. Shi, W. Xu, T.-H. Chang, Y. Wang, and E. Song, "Joint beamforming and power splitting for MISO interference channel with SWIPT: An SOCP relaxation and decentralized algorithm," *IEEE Trans. Signal Process.*, vol. 62, no. 23, pp. 6194–6208, Dec. 2014.
- [38] H. Lee, S.-R. Lee, K.-J. Lee, H.-B. Kong, and I. Lee, "Optimal beamforming designs for wireless information and power transfer in MISO interference channels," *IEEE Trans. Wireless Commun.*, vol. 14, no. 9, pp. 4810–4821, Sep. 2015.
- [39] S. Goel and R. Negi, "Guaranteeing secrecy using artificial noise," *IEEE Trans. Wireless Commun.*, vol. 7, no. 6, pp. 2180–2189, Jun. 2008.
- [40] X. Zhou and M. R. McKay, "Secure transmission with artificial noise over fading channels: Achievable rate and optimal power allocation," *IEEE Trans. Veh. Technol.*, vol. 59, no. 8, pp. 3831–3842, Oct. 2010.
- [41] D. W. K. Ng, E. S. Lo, and R. Schober, "Robust beamforming for secure communication in systems with wireless information and power transfer," *IEEE Trans. Wireless Commun.*, vol. 13, no. 8, pp. 4599–4615, Aug. 2014.
- [42] J. Zhu, R. Schober, and V. K. Bhargava, "Linear precoding of data and artificial noise in secure massive MIMO systems," *IEEE Trans. Wireless Commun.*, vol. 15, no. 3, pp. 2245–2261, Mar. 2016.
- [43] Y. Chen *et al.*, "Why time reversal for future 5G wireless? [Perspectives]," *IEEE Signal Process. Mag.*, vol. 33, no. 2, pp. 17–26, Mar. 2016.
- [44] Z.-H. Wu, Y. Han, Y. Chen, and K. J. R. Liu, "A time-reversal paradigm for indoor positioning system," *IEEE Trans. Veh. Technol.*, vol. 64, no. 4, pp. 1331–1339, Apr. 2015.
- [45] C. Chen, Y. Chen, Y. Han, H.-Q. Lai, and K. J. R. Liu, "Achieving centimeter-accuracy indoor localization on WiFi platforms: A frequency hopping approach," *IEEE Internet Things J.*, vol. 4, no. 1, pp. 111–121, Feb. 2017.
- [46] C. Chen, Y. Chen, H.-Q. Lai, Y. Han, and K. J. R. Liu, "High accuracy indoor localization: A WiFi-based approach," in *Proc. IEEE Int. Conf. Acoust. Speech Signal Process. (ICASSP)*, Shanghai, China, Mar. 2016, pp. 6245–6249.
- [47] F. Zhang, C. Chen, B. Wang, H.-Q. Lai, and K. J. R. Liu, "A time-reversal spatial hardening effect for indoor speed estimation," in *Proc. IEEE Int. Conf. Acoust. Speech Signal Process.*, New Orleans, LA, USA, Mar. 2017, pp. 5955–5959.
- [48] Q. Xu, Y. Chen, B. Wang, and K. J. R. Liu, "TRIEDS: Wireless events detection through the wall," *IEEE Internet Things J.*, vol. 4, no. 3, pp. 723–735, Jun. 2017.
- [49] Q. Xu, Y. Chen, B. Wang, and K. J. R. Liu, "Radio biometrics: Human recognition through a wall," *IEEE Trans. Inf. Forensics Security*, vol. 12, no. 5, pp. 1141–1155, May 2017.
- [50] C. Chen, Y. Han, Y. Chen, and K. J. R. Liu, "Multi-person breathing rate estimation using time-reversal on WiFi platforms," in *Proc. IEEE Glob. Conf. Signal Inf. Process.*, Washington, DC, USA, Dec. 2016, pp. 1059–1063.
- [51] B. Bogert, "Demonstration of delay distortion correction by time-reversal techniques," *IRE Trans. Commun. Syst.*, vol. 5, no. 3, pp. 2–7, Dec. 1957.
- [52] F. Wu, J.-L. Thomas, and M. Fink, "Time reversal of ultrasonic fields. II. Experimental results," *IEEE Trans. Ultrason., Ferroelect., Freq. Control*, vol. 39, no. 5, pp. 567–578, Sep. 1992.
- [53] C. Dorme, M. Fink, and C. Prada, "Focusing in transmit-receive mode through inhomogeneous media: The matched filter approach," in *Proc. IEEE Ultrasonics Symp.*, vol. 1, Tucson, AZ, USA, Oct. 1992, pp. 629–634.
- [54] A. Derode, P. Roux, and M. Fink, "Acoustic time-reversal through high-order multiple scattering," in *Proc. IEEE Ultrasonics Symp. Int.*, vol. 2, Seattle, WA, USA, Nov. 1995, pp. 1091–1094.
- [55] W. A. Kuperman *et al.*, "Phase conjugation in the ocean: Experimental demonstration of an acoustic time-reversal mirror," *J. Acoust. Soc. America*, vol. 103, no. 1, pp. 25–40, 1998.
- [56] D. Rouseff *et al.*, "Underwater acoustic communication by passive-phase conjugation: Theory and experimental results," *IEEE J. Ocean. Eng.*, vol. 26, no. 4, pp. 821–831, Oct. 2001.
- [57] G. F. Edelmann *et al.*, "An initial demonstration of underwater acoustic communication using time reversal," *IEEE J. Ocean. Eng.*, vol. 27, no. 3, pp. 602–609, Jul. 2002.
- [58] B. E. Henty and D. D. Stancil, "Multipath-enabled super-resolution for RF and microwave communication using phase-conjugate arrays," *Phys. Rev. Lett.*, vol. 93, no. 24, 2004, Art. no. 243904.
- [59] G. Lerosey *et al.*, "Time reversal of electromagnetic waves," *Phys. Rev. Lett.*, vol. 92, no. 19, 2004, Art. no. 193904.
- [60] G. Lerosey *et al.*, "Time reversal of electromagnetic waves and telecommunication," *Radio Sci.*, vol. 40, no. 6, pp. 1–10, 2005.
- [61] G. Lerosey, J. De Rosny, A. Tourin, A. Derode, and M. Fink, "Time reversal of wideband microwaves," *Appl. Phys. Lett.*, vol. 88, no. 15, 2006, Art. no. 154101.
- [62] J. de Rosny, G. Lerosey, and M. Fink, "Theory of electromagnetic time-reversal mirrors," *IEEE Trans. Antennas Propag.*, vol. 58, no. 10, pp. 3139–3149, Oct. 2010.
- [63] I. H. Naqvi *et al.*, "Experimental validation of time reversal ultra wide-band communication system for high data rates," *IET Microw. Antennas Propag.*, vol. 4, no. 5, pp. 643–650, May 2010.
- [64] M. Emami, M. Vu, J. Hansen, A. J. Paulraj, and G. Papanicolaou, "Matched filtering with rate back-off for low complexity communications in very large delay spread channels," in *Proc. 38th Asilomar Conf. Signals Syst. Comput.*, Pacific Grove, CA, USA, 2004, pp. 218–222.
- [65] Q. Xu, Y. Chen, and K. J. R. Liu, "Optimal pricing for interference control in time-reversal device-to-device uplinks," in *Proc. IEEE Glob. Conf. Signal Inf. Process. (GlobalSIP)*, Orlando, FL, USA, Dec. 2015, pp. 1096–1100.
- [66] T. K. Y. Lo, "Maximum ratio transmission," *IEEE Trans. Commun.*, vol. 47, no. 10, pp. 1458–1461, Oct. 1999.
- [67] T. L. Marzetta, "Noncooperative cellular wireless with unlimited numbers of base station antennas," *IEEE Trans. Wireless Commun.*, vol. 9, no. 11, pp. 3590–3600, Nov. 2010.
- [68] A. Goldsmith, *Wireless Communications*. Cambridge, U.K.: Cambridge Univ. Press, 2005.
- [69] Q. H. Spencer, A. L. Swindlehurst, and M. Haardt, "Zero-forcing methods for downlink spatial multiplexing in multiuser MIMO channels," *IEEE Trans. Signal Process.*, vol. 52, no. 2, pp. 461–471, Feb. 2004.
- [70] S. Shi, M. Schubert, and H. Boche, "Rate optimization for multiuser MIMO systems with linear processing," *IEEE Trans. Signal Process.*, vol. 56, no. 8, pp. 4020–4030, Aug. 2008.
- [71] D. N. C. Tse and P. Viswanath, "Downlink-uplink duality and effective bandwidths," in *Proc. IEEE Int. Symp. Inf. Theory*, Lausanne, Switzerland, 2002, p. 52.
- [72] T. Ma, Q. Shi, and E. Song, "QoS-constrained weighted sum-rate maximization in multi-cell multi-user MIMO systems: An ADMM approach," in *Proc. 35th Chin. Control Conf. (CCC)*, Chengdu, China, Jul. 2016, pp. 6905–6910.
- [73] M. Schubert and H. Boche, "Solution of the multiuser downlink beamforming problem with individual SINR constraints," *IEEE Trans. Veh. Technol.*, vol. 53, no. 1, pp. 18–28, Jan. 2004.
- [74] J. Wang and D. P. Palomar, "Worst-case robust MIMO transmission with imperfect channel knowledge," *IEEE Trans. Signal Process.*, vol. 57, no. 8, pp. 3086–3100, Aug. 2009.
- [75] F. Zhang, "Report for optimization-based pinpoint beamforming," Univ. Maryland, at College Park, College Park, MD, USA, Tech. Rep., Jul. 2015.
- [76] L. R. Varshney, "Transporting information and energy simultaneously," in *Proc. IEEE Int. Symp. Inf. Theory*, Toronto, ON, Canada, Jul. 2008, pp. 1612–1616.
- [77] X. Lu, P. Wang, D. Niyato, D. I. Kim, and Z. Han, "Wireless networks with RF energy harvesting: A contemporary survey," *IEEE Commun. Surveys Tuts.*, vol. 17, no. 2, pp. 757–789, 2nd Quart., 2015.
- [78] P. Grover and A. Sahai, "Shannon meets Tesla: Wireless information and power transfer," in *Proc. IEEE Int. Symp. Inf. Theory*, Austin, TX, USA, Jun. 2010, pp. 2363–2367.
- [79] X. Zhou, R. Zhang, and C. K. Ho, "Wireless information and power transfer: Architecture design and rate-energy tradeoff," *IEEE Trans. Commun.*, vol. 61, no. 11, pp. 4754–4767, Nov. 2013.
- [80] K. Huang and E. Larsson, "Simultaneous information and power transfer for broadband wireless systems," *IEEE Trans. Signal Process.*, vol. 61, no. 23, pp. 5972–5986, Dec. 2013.

- [81] M. Tian, X. Huang, Q. Zhang, and J. Qin, "Robust AN-aided secure transmission scheme in MISO channels with simultaneous wireless information and power transfer," *IEEE Signal Process. Lett.*, vol. 22, no. 6, pp. 723–727, Jun. 2015.



**Qinyi Xu** (S'15) received the B.S. (Highest Hons.) degree in information engineering from Southeast University, Nanjing, China, in 2013. She is currently pursuing the Ph.D. degree with the Department of Electrical and Computer Engineering, University of Maryland College Park, MD, USA. Her current research interests include signal processing and wireless communications.

She was an exchange student with the KTH-Royal Institute of Technology, Stockholm, Sweden, from 2012 to 2013, with the national sponsorship of China. She was a recipient of the Clark School Distinguished Graduate Fellowships from University of Maryland, College Park, and the Graduate with Honor Award from Southeast University in 2013.



**Chunxiao Jiang** (S'09–M'13–SM'15) received the B.S. (Highest Hons.) degree in information engineering from Beihang University in 2008 and the Ph.D. (Highest Hons.) degree in electronic engineering from Tsinghua University in 2013. From 2013 to 2016, he was a Post-Doctoral Researcher with the Department of Electronic Engineering, Tsinghua University, during which he visited the University of Maryland College Park. He is currently a Research-Track Faculty Member, an Assistant Research Fellow with Tsinghua Space Center,

Tsinghua University. He was a recipient of the IEEE Globecom Best Paper Award in 2013, the IEEE GlobalSIP Best Student Paper Award in 2015, and the IEEE Communications Society Young Author Best Paper Award in 2017.



**Yi Han** received the B.S. (Highest Hons.) degree in electrical engineering from Zhejiang University, Hangzhou, China, in 2011 and the Ph.D. degree from the Department of Electrical and Computer Engineering, University of Maryland, College Park, in 2016. He is currently the Wireless Architect of Origin Wireless. His research interests include wireless communication and signal processing.

Dr. Han was a recipient of the Class A Scholarship from Chu Kochen Honors College, Zhejiang University, in 2008 and the Best Student Paper Award of IEEE ICASSP in 2016.



**Beibei Wang** (SM'15) received the B.S. (Highest Hons.) degree in electrical engineering from the University of Science and Technology of China, Hefei, in 2004 and the Ph.D. degree in electrical engineering from the University of Maryland, College Park, in 2009. She was with the University of Maryland as a Research Associate from 2009 to 2010, and with Qualcomm Research and Development from 2010 to 2014. Since 2015, she has been with Origin Wireless Inc., where she is currently a Chief Scientist in Wireless. She has

co-authored the book entitled *Cognitive Radio Networking and Security: A Game-Theoretic View* (Cambridge University Press, 2010). Her research interests include wireless communications and signal processing. She was a recipient of the Graduate School Fellowship, the Future Faculty Fellowship, and the Dean's Doctoral Research Award from the University of Maryland, and the Overview Paper Award from IEEE Signal Processing Society in 2015.



**K. J. Ray Liu** (F'03) was named a Distinguished Scholar-Teacher with the University of Maryland, College Park, in 2007, where he is a Christine Kim Eminent Professor of information technology. He leads the Maryland Signals and Information Group conducting research encompassing broad areas of information and communications technology with recent focus on smart radios for smart life.

He was a recipient of the 2016 IEEE Leon K. Kirchmayer Technical Field Award on graduate teaching and mentoring, the IEEE Signal Processing Society 2014 Society Award, the IEEE Signal Processing Society 2009 Technical Achievement Award, and the Highly Cited Researcher Award by Thomson Reuters. He is a fellow of AAAS.

Dr. Liu is a member of IEEE Board of Director as the Division IX Director. He was the President of IEEE Signal Processing Society, where he has served as the Vice President—Publications and Board of Governor. He has also served as the Editor-in-Chief of the *IEEE Signal Processing Magazine*.

He also received teaching and research recognitions from the University of Maryland, including the University-Level Invention of the Year Award, the College-Level Poole and Kent Senior Faculty Teaching Award, the Outstanding Faculty Research Award, and the Outstanding Faculty Service Award, all from A. James Clark School of Engineering.